Optimizing the Selection of COVID-19 Vaccine Distribution Centers and Allocation Quantities:

A Case Study for the County of Los Angeles

By

Basim Masad Aljohani

A Thesis Presented to the
FACULTY OF THE USC VITERBI SCHOOL OF ENGINEERING
UNIVERSITY OF SOUTHERN CALIFORNIA
In Partial Fulfillment of the
Requirements for the Degree
MASTER OF SCIENCE
(INDUSTRIAL AND SYSTEMS ENGINEERING)

August 2023

[[And certainly did WE create man from an extract of clay ۞ Then WE placed him as a sperm-drop in a firm lodging ۞Then WE made the sperm-drop into a clinging clot, and WE made the clot into a lump [of flesh], and WE made [from] the lump, bones and WE covered the bones with flesh; then WE developed him into another creation. So blessed be Allah, the best of creators]]

- Holy Quran, Chapter 23, verses 12 through 14

A dedication to my inspiration and role model, my father, Masad Aljohani:

I would not be the man I am today without you and the lessons you taught me. Thank you for everything you have done to make my life better and easier. Your absence has left me with an unfillable void. I miss you deeply, and I pray to Almighty Allah to grant you the highest levels of paradise.

Acknowledgments

First, all praise is due to Allah the Almighty, the most gracious and the most merciful, for his blessing and guidance throughout my life, during my study, and in completing my thesis.

I would like to express my deepest gratitude and sincere thanks to my advisor, Dr. Randolph Hall, for his valuable support, guidance, and deep knowledge, which have been extremely valuable and helpful throughout my research journey. The skills and knowledge I have acquired working with you are invaluable assets that will undoubtedly help me in my future. Thanks are also extended to King Fahd University of Petroleum and Minerals for providing me with a scholarship to continue my graduate education.

I would like to extend my sincere gratitude to my thesis committee members: Dr. Sze-chuan Suen and Dr.Andres Gomez. I am very appreciative and grateful for the time and effort you devoted to reviewing my thesis and for being on my committee.

Thanks are also extended to Mingdong Lyu for his valuable feedback and support throughout my thesis journey.

Last, but certainly not least, I would like to express my heartfelt gratitude to my family, whose continuous support has always been a source of strength throughout my life. To my dear mother, whose endless love and encouragement have inspired me to strive for excellence and helped make me the man I am today. To my loving wife, Mawaddah, thank you for always believing in me and for your support during times of stress. Your patience during the long times I was away busy working is sincerely appreciated. And to my siblings, Nahla, Mohammed, Khalid, Tawfiq, Fahad, and Norah, thank you for always being there when I needed someone to lean on. Your support and love have always been a source of constant inspiration.

Table of Contents

Epigraph ii
Dedication iii
Acknowledgments iv
List of Tables vii
List of Figures vii
List of Maps viii
Abstract ix
Chapter One: Introduction 1
1.1 Background and Context of the Study 1
1.2 Research Objectives and Question 3
Chapter Two: Literature Review 5
2.1 Review on the Special Analysis of Vaccine Distribution 5
2.2 Review on Optimization of the COVID-19 Vaccine Centers Locations 7
2.3 Review on Allocation of the COVID-19 Vaccines 10
Chapter Three: Methodology 16
3.1 Travel Time and Distance. 16
3.2 Optimization Model. 17
3.2.1 Model Sets, Parameters, and Decision Variables. 18
3.2.2 Objective Function and Constraints 19
3.3 Modeling The Different Scenarios 22
3.3.1 Scenario One: Prioritizing Areas Based on Population. 22
3.3.2 Scenario Two: Prioritizing Areas Based on the Healthy Places Index. 22
3.3.3 Scenario Three: Prioritizing Areas Based on the Vulnerability to Covid-19. 23
Chapter Four: Study Area and Datasets 27
4.1 Los Angeles County Metropolitan Area. 27
4.2 Datasets 29
4.2.1 Demographic Data 29
4.2.2 Healthy Places Index 29
4.2.3 Covid-19 Data 30
4.2.4 Vulnerability to Covid-19 30
4.2.5 Car Ownership Data 30

4.2.6 Geographical Data 31
Chapter Five: Results and Discussion. 32
5.1 Model Output for Optimal Vaccine Distribution Sites. 32
5.1.1 Scenario One: 32
5.1.2 Scenario Two: 35
5.1.3 Scenario Three: 36
5.2 Model Output Optimal Vaccine Distribution Sites: 38
5.2.1 Scenario One: 38
5.2.2 Scenario Two: 39
5.2.3 Scenario Three: 39
5.3 Sensitivity Analysis. 41
5.3.1 Changing the Maximum Number of Sites 41
5.3.2 Changing the Number of Sites Residents Can Choose From (F). 44
5.4 Comparison Between the Optimal Sites vs the Actual LA County Vaccine Sites 47
5.5 Limitations 52
Chapter Six: Conclusion. 53
6.1 Summary of Findings. 53
6.2 Contributions to the Field. 55
6.3 Future Research. 56
References 57
Appendix 61

List of Tables

Table 1: Car travel time matrix in minutes 17
Table 2: Wi calculations using HPI 23
Table 3: Racial vulnerability to Covid-19 by CDC 24
Table 4: Risks scores calculations example for zip code 90029 25
Table 5: Weights for risks measures 26
Table 6: Optimal costs breakdown 32
Table 7: Optimal costs breakdown for scenario 2 35
Table 8: Optimal costs breakdown for scenario 3 36
Table 9: Summary of cost types for all scenarios 37
Table 10: average travel times and distance values for all scenarios 40
Table 11: Total cost for different max sites for all scenarios 43
Table 12: Total cost weighted by HPI for different max sites for all scenarios 43
Table 13: Total cost weighted by COVID-19 Vulnerability Index for different max sites 44
Table 14: Total weighted costs for different F values for all scenarios 46
Table 15: Loop output for scenario 1 66
Table 16: Loop output for scenario 2 68
Table 17: Loop output for scenario 3 70

List of Figures

Figure 1: Vaccination uptake rates in LA County according to LA Public Health[1] 2
Figure 2: Scatterplot of average travel time by transit vs population of zip codes 33
Figure 3: Scatterplot of average travel time by car vs the population of zip codes 34
Figure 4: Scatterplot of average distance vs the population of zip codes 34
Figure 5: Box plot of HPI percentile for selected sites 36
Figure 6: Cost types vs number of maximum sites 41
Figure 7: Average travel times and distance vs max sites 42
Figure 8: Average travel times and distance comparison 49
Figure 9: Cost types comparison 50
Figure 10: Average travel times and distance comparison 51
Figure 11: Cost types comparison 51
Figure 12: Cost types vs max sites for scenario 2 61
Figure 13: Average travel times and distance vs max sites for scenario 2 61
Figure 14: Cost types vs max sites for scenario 3 63
Figure 15: Average travel times and distance vs max sites for scenario 2 63

List of Maps

Map 1: LA County population heatmap 28
Map 2: Map of optimal sites for the first scenario 33
Map 3: Map of optimal sites for the second scenario 35
Map 4: Map of optimal sites for third scenario 37
Map 5: Vaccine allocation for the first scenario 38
Map 6: Vaccine allocation for the second scenario 39
Map 7: Vaccine allocation for the third scenario 40
Map 8: Map of optimal sites when F=1 45
Map 9: Map of optimal sites when F=5 45
Map 10: Map of the actual vaccine sites in LA county 48
Map 11: Map of selected sites when F=1, scenario 2 62
Map 12: Map of selected sites when F=5, scenario 2 62
Map 13: Optimal sites for F=1, scenario 3 64
Map 14: Optimal sites for F=5, scenario 3 64

Abstract

This thesis aims to provide a tool to help policy and decision-makers establish well-informed plans about the selection and distribution of locations and quantities of vaccines. Optimization of vaccine distribution centers' locations plays a crucial role in providing communities with easy access to vaccines, which will help in controlling global pandemics, such as the recent COVID-19, and mitigate the risks of losing lives and economic losses. As studies have proven, strategic planning of the vaccine site locations and the allocated quantities of the vaccines could help boost the amount of vaccine uptake. This thesis utilizes mathematical modeling techniques to develop a mixed integer program that aims to minimize travel time, distance, and associated costs in one of the largest counties in the United States, Los Angeles County. The developed model takes into account the diverse demographics and socioeconomic factors of the County and plans for the selection and allocations accordingly. The model explores 277 zip codes within Los Angeles and analyzes them as potential vaccine distribution centers. It also incorporates the two different and most common means of transportation, cars, and public transit, to account for all users. Three scenarios are explored where each zip code of the 277 is assigned priority based on the following factors: population, Healthy Places Index, and a Vulnerability to COVID-19 index. The output showed significant improvements in reducing average travel times and distances as well as savings in costs when compared to the actual selected sites within the County.

Chapter One: Introduction

1.1 Background and Context of the Study

The coronavirus disease 2019 (COVID-19) emerged as a global threat in late 2019, quickly evolving into a pandemic that has deeply impacted every aspect of modern life. The rapid spread of the virus across the globe has placed massive pressure on healthcare systems, disrupted economies, and altered social norms. Governments, organizations, and individuals have been forced to adapt to new challenges and find innovative solutions in order to save lives and minimize any economic losses.

In response to the crisis, researchers and pharmaceutical companies worldwide have worked tirelessly to develop vaccines and medicine to combat the virus. The rapid development and distribution of COVID-19 vaccines have been critical in mitigating the pandemic's impact and making way for a gradual return to everyday life. Strategically choosing the sites to administer the vaccines and planning the allocation of the quantities have become a top priority to ensure smooth delivery to vulnerable populations and regions with limited resources in order to receive the protection they need.

In this context, the study of sites selection and vaccines distribution, particularly in densely populated and diverse regions like the Los Angeles (LA) County metropolitan area, is of major importance. By optimizing the location of vaccine distribution centers while considering important factors such as travel time, distances, costs, and the demographics of the populations, this research aims to contribute to more efficient and equitable vaccine accessibility, ultimately improving public health outcomes in the face of ongoing global challenges.

The Los Angeles County metropolitan area is among the most densely populated and diverse regions in the United States. It comprises many urban, suburban, and rural areas, each exhibiting distinct demographic and health characteristics. With a population of over 10 million people dispersed across roughly 4,000 square miles, LA County confronts substantial logistical obstacles in vaccine distribution. According to LA County Department of Public Health [1] data, as of June 11th, 2023, around 8.33 million residents (81% of total LA county population) are vaccinated with at least a single dose, and 7.56 million (74%) are fully vaccinated. While these numbers might appear high, higher vaccination rates are desired in order to contain the severe risks of the virus.

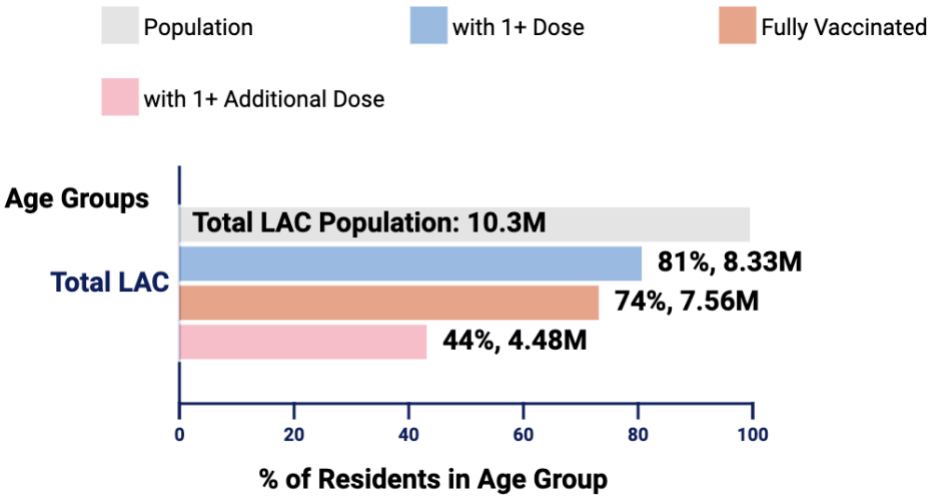

Figure 1: Vaccination uptake rates in LA County according to LA Public Health[1]

These challenges are further aggravated by inequalities in health outcomes and access to healthcare services across different communities within the County. Socioeconomic aspects, environmental factors, and healthcare infrastructure contribute to an uneven distribution of health risks and resources in the region. For instance, areas with lower socioeconomic status might face a higher prevalence of chronic diseases or limited access to healthcare facilities, amplifying the importance of strategically choosing the locations of the sites and efficiently distributing the vaccine.

Moreover, incorporating health indices like the Healthy Places Index (HPI) allows for a more targeted approach, prioritizing areas with greater health disparities and vulnerabilities. This ensures that those most in need receive vital immunizations in a timely manner, contributing to a more equitable distribution of resources and improved public health outcomes.

In summary, this study aims to identify optimal locations for vaccine distribution centers in the LA County metropolitan area by considering a range of factors, including travel time, costs, and health indices. By doing so, it seeks to promote more cost-efficient and equitable access to vaccines, ultimately leading to improved public health outcomes for the diverse communities within the region while maintaining the minimum possible costs.

1.2 Research Objectives and Question

The primary aim of this study is to formulate a well-informed strategy for identifying the most suitable locations for vaccine distribution centers within the Los Angeles County metropolitan area. By considering a range of factors such as travel duration, costs, health indicators, and ease of access, the study aspires to advance the effectiveness and fairness of vaccine distribution across the region's varied communities as well as keeping the costs to a minimum.

An essential part of this research is identifying which critical variables should be taken into account when deciding on the best locations for vaccine distribution centers. These variables need to be integrated into a comprehensive framework that strikes a balance between efficiency, equity, and accessibility, thereby enhancing the vaccine distribution process for all residents. The investigation will incorporate health indicators, such as the HPI index, into the location strategy. This inclusion aims to give priority to areas with higher health disparities and susceptibilities.

Through addressing these research focus areas, the study hopes to offer valuable insights and strategic recommendations for public health authorities, policymakers, and other parties involved in organizing and executing vaccine distribution efforts. The wider implications of the proposed strategy concerning public health and emergency preparedness in urban, suburban, and rural settings will also be assessed. Ultimately, the research seeks to foster more cost-efficient and equitable vaccine distribution, improving public health outcomes for the diverse communities within the Los Angeles County metropolitan area and beyond.

Chapter Two: Literature Review

Optimization models have been increasingly utilized in the healthcare sector to improve health outcomes and increase efficiency and effectiveness. Applications include resource allocations and strategic planning of healthcare facilities' locations, especially in times of global pandemics such as the recent COVID-19. In the case of vaccine distribution and optimal selection of vaccine centers, optimization models can help determine the most effective ways to distribute the vaccines to achieve the maximum converge and reduce the impact of the pandemic. In the context of this thesis, the following sections will explore the progress recent research has achieved in the analysis of accessibility, optimization of facility and vaccine administration locations, and allocations of vaccines using mathematical modeling.

2.1 Review on the Special Analysis of Vaccine Distribution

Spatial analysis and accessibility have been a major part of the research conducted on vaccine distribution as it helps identify disparities in vaccination rates and areas with highly vulnerable population groups. One comprehensive spatial analysis was conducted by Mollalo, Mohammadi, Mavaddati, and Kiani (2021) [2] in their paper "Spatial Analysis of COVID-19 Vaccination: A Scoping Review", which summarized previous findings and highlighted research gaps. They also concluded that significant geographic disparities in COVID-19 vaccination rates are present, with some regions and countries having higher rates, which they attribute to factors such as having access to more supply and healthcare services, as well as the presence of vaccine hesitancy. This comprehensive study provided an excellent overview on the topic and facilitated the search for previous studies relevant to this thesis. In another study, "Spatial Modeling of COVID-19 Vaccine Hesitancy in the United States", by Mollalo and Tatar (2021) [3], the authors presented a GIS-based study to analyze the spatial heterogeneity of COVID-19 vaccination rates across all counties

in the United States using Social Vulnerability Index (SVI) data. The study utilized regression models, such as the Ordinary Least Squares and Geographically Weighted Regression models, to study the relationship between the socioeconomic factors of the counties and their achieved vaccination rates. Such application of regression tools could be utilized to study the relationships between COVID-19 deaths and the demographics of the zip codes within the scope of this thesis, to enhance establishing more targeted vaccine distribution strategies. Moreover, the paper "The Use of GIS Technology to Optimize COVID-19 Vaccine Distribution: A Case Study of the City of Warsaw, Poland" by Krzysztofowicz and Osinska-Skotak (2021) [4], the authors utilized GIS technology to visualize the spatial distributions and patterns, which could be crucial for understanding and determining the sites that have the maximum reach and efficiency. The tool also assisted them in identifying the areas with higher populations of age groups eligible to receive the vaccines, which helped achieve a more targeted vaccination campaign.

In another study, by Alemdar, Kaya, Çodur, Campisi, and Tesoriere (2021) [5], the authors highlighted the importance of the logistics of the vaccines and the selection process of the sites for dispensing vaccines. They proposed a three-step solution for site selection, where they defined eight evaluation criteria based on the suggestion of advisory boards, assigned a weight to each criterion, and finally assigned potential sites and determined service areas by obtaining a suitability map. Building upon these previous studies, this thesis extends the strategic selection of vaccination sites by the inclusion of additional factors such as travel times, populations, and costs into the optimization model, which leads to a more comprehensive tool for decision-makers. Lastly, spatial accessibility to urban medical facilities in China was assessed by Cheng, Tao, Lian, and Huang (2021) [6], where they used a comprehensive transportation network composed of ground transportation and rail transit and calculated the spatial accessibility of small units. They adopted

empirical Kriging interpolation methods as well as cluster and outlier analysis, concluding that poor accessibility was presented in most of their study area and that residential areas along the subway had better access to the facilities. In the end, the authors proposed that improving the transportation network leads to overall better medical facility accessibility.

2.2 Review on Optimization of the COVID-19 Vaccine Centers Locations

The topic of COVID-19 vaccine center locations has emerged as significant area of study since the global pandemic emerged in 2020. Numerous studies have employed mathematical modeling techniques, incorporating various factors such as travel times, distances, and operational costs to identify optimal locations that would help reduce the impact of the pandemic. A study by Bravo, Hu, and Long (2022) [7], [8] considered travel distance when optimizing the selection of vaccines. The authors argue that reducing the travel distances can improve vaccination rates, where they proposed using retail pharmacies and dollar stores as vaccination sites to reduce the disparities across demographic groups. This reduction allows for an additional 25% of the population to be within walking distance (<1 Km) of a vaccine site. Moreover, they concluded that an increase of 5% in vaccinations would be achieved by applying the pharmacy and dollar stores strategy. However, this paper incorporated Euclidian distance between populations centroid and locations in their model whereas this thesis explores traveled distance in a more accurate approach using Maps API, which yields real life like travel times and distances. Similarly, using a facility location optimization model and travel estimates from the US National Household Travel Survey data, the authors Risanger, Singh, Morton, and Meyers (2021) [9] introduced a function calculating the fractions of populations willing to travel, where it showed different behaviors for trip distances above and below 5 miles. Such application of functions could be helpful when deciding on the locations of public health facilities and vaccination sites. Their model is formulated to maximize

the population willing to travel to its closest site based on their introduced travel willingness function with the assumption that there is a maximum number of locations that can be selected, unlike what the introduced model in this thesis tris to achieve which is to minimize the travel distance and time between populations and locations. In another study, Bertsimas, Digalakis Jr, Jacquillat, Li, and Previero (2021) [10] proposed an epidemiological model called DELPHI and integrated it into an optimization model that plans strategic vaccine distributions. Their approach starts by forecasting the dynamic of the pandemic using an SEIR model and then it accounts for the vaccination impact on the populations based on the vaccine effectiveness. Lastly, these inputs are then integrated into a model used to optimize the vaccine distribution strategy, which increases the effectiveness of the vaccination campaign by an estimated 20%, which is projected to save an extra 4000 lives in the United States within three months. Unlike the SEIR model, this thesis takes another approach and explores a distribution strategy based on prioritization criteria that can be selected by decision makers.

Points of Dispensing (PODs) were also proposed in a study by Alghanmi, Alotaibi, Alshammari, Alhothali, Bamasag, and Faisal (2022) [11], where the authors discussed the importance of PODs during public health emergencies. They presented a survey of PODs location-allocation models, where various optimization models were discussed which included minimizing maximum travel times, minimizing total weighted travel time and distance, and the associated costs. This thesis extends this work by analyzing adding more flexibility to the model, where demand points could have more than one option of facilities to receive the vaccines. Furthermore, minimizing the traveled distance is also discussed by Lusiantoro, Mara, and Rifai (2022) [12], which they incorporated in their bi-objective linear programming model. They aimed at maximizing the coverage for vaccine recipients while also minimizing the weighted distance travelled. They

applied the model to Yogyakarta of Indonesia, and their results suggested that prioritizing areas with high COVID-19 cases caused less efficient coverage, which suggests that other factors beyond the cases might need to be considered, which is considered in the developed model in this thesis, where decision makers have the choice to select from multiple prioritization criteria. Another multi-objective optimization model was proposed by Tang, Li, Bai, Liu, and Coelho (2022) [13], where the authors tried to optimize the operational costs of vaccine sites and the total travel distance for multi-period COVID-19 vaccination planning. A decision framework was also proposed to help decision-makers choose based on real-life limitations or preferences while optimizing the service level. The results of the model showed a 9.3% decrease in the operational cost and a 36.6% decrease in the total traveled distance. Our work builds on this by considering other costs such as the travel time, cost of public transit, and cost of traveled distance into the objective function. At a municipality level, Cabanilla, Enriquez, Mendoza, and Mendoza (2022) [14] presented optimal locations of vaccine sites, where they considered existing public facilities, such as hospitals and schools, as potential sites. They divided the town into several smaller areas and assigned weights to densely populated and highly contagious areas with higher case counts. After that, they incorporated those weighting factors into a distance minimization problem between the sites and the areas of the town. This thesis extends this work by considering every area in the study as a potential site and by incorporating different means of transportation into the model. Furthermore, a Location-Allocation model was developed by Faisal, Alshammari, Alotaibi, Alghanmi, Bamsagm, and Bin Yamin (2022) [15] to improve the distribution of COVID-19 vaccine centers in Jeddah, Saudi Arabia. The authors introduced a maximal coverage model with and without facility capacity constraints. They applied the model with different impedance cutoffs, which are the maximum travel times required from demand points to vaccine centers. Moreover,

the authors explored the minimum number of facilities needed to satisfy all the demand points within the city by minimizing the overall transportation time and distance.

2.3 Review on Allocation of the COVID-19 Vaccines

As we dive into the third section of the literature review, we shift our focus to vaccine allocation, particularly through the lens of optimization techniques. During times of emergencies, like the COVID-19 pandemic, equitable distribution of the vaccines is essential to ensure that all populations, especially the most vulnerable, have access. This is a complex task that requires the use of advanced mathematical modeling and optimization techniques to mitigate pandemics.

We first need to understand the relationship between the different characteristics of communities and COVID-19 vulnerability and death rates. This was explored by Karmakar, Lantz, and Tipirneni (2021) [16], where the authors analyzed the association between the US county-level sociodemographic factors and COVID-19 incidence and mortality using a mixed-effects negative binomial regression. They used the SVI as a measure of community vulnerability to the virus and found a significant correlation between the two. Moreover, Ong, Pech, Gutierrez, and Mays (2021) [17] presented in their paper "COVID-19 Medical Vulnerability Indicators: A Predictive, Local Data Model for Equity in Public Health Decision Making", a study that aimed to develop a predictive model of the vulnerability indicators for COVID-19 in Los Angeles County using four key indicators to capture the dimensions of COVID-19 related vulnerabilities. The indicators were pre-existing health conditions, barriers to accessing healthcare, built environment risks, and the SVI. The study concluded that the racial groups of LatinX, Blacks and segments of the Asian populations were the most vulnerable to COVID-19. Building on this, this thesis uses similar social

characteristics in the optimization of sites locations, where it ensures equitability by addressing the communities that are most vulnerable.

Many research papers have addressed fairness and equality in allocations of vaccines, as in Balcik, Yucesoy, Akca, Karakaya, Gevsek, Baharmand and Sgarbossa (2022) [18]. The authors presented a mathematical model that is designed to find an effective and equitable allocation plan while prioritizing vulnerable groups and regions. Their objective function is to minimize the weighted sum of deviations (both positive and negative) from the fair coverage levels while also minimizing the deviation for the coverage threshold for certain groups by penalizing this deviation. The model achieved a 74% coverage, which is very close to the ratio of total supply to total demand (74.93%). In another paper by Anaahideh, Kang, and Nezami (2022) [19], the authors tried to achieve a fair allocation plan in terms of demographic disparity by maximizing geographical diversity while also maximizing fairness among certain groups of the population. They designed a multi-objective optimization model that minimizes the weighted sum of deviation from the fair coverage levels to ensure that the allocation is fair and diverse across different geographical and social groups. They defined geographical diversity by a standard that all centers of vaccine should have the same average amount of resources per capita regardless of location, which helps achieve an evenly spread-out distribution of resources. The social fairness in their paper is defined by the standard that for every social group, the average amount of resources allocated per capita should not vary depending on the socioeconomic attributes of the groups. In addition, Wang (2021) [20] analyzed data visualization and optimization to achieve an equitable distribution of COVID-19 vaccines. He analyzed demographic data, such as population, race, age, and socioeconomic data, such as poverty and unemployment, using business analytics tools to identify trends, such as regions with high probability needs for hospitalization. He then integrated his optimization model to determine

the optimal cost-efficient method of allocations using the trends and patterns identified. His results suggested an allocation plan that leans towards the areas in most need to ensure equitability.

One more contribution to the literature on the field of fair allocation of resources was made by Singh (2020) [21]. The author presented a math model to analyze the allocation of resources based on a set of user groups and a set of resource types while also considering the abundance of those resources. The study concluded that if a resource is abundant, all users will achieve the maximum possible coverage, whereas if it was scarce, the allocation will be equitable across all the user groups. Taking inspiration from these studies, this thesis incorporates giving priority to vulnerable groups and demographics of each zip code within the study area, which helps achieve a more efficient health outcomes.

Similarly, other contributions to the field of vaccine allocation focused on specific goals, such as minimizing the death counts caused by the virus, as studied by the authors of [22]. The study utilized a constrained optimization model that aimed to minimize the projected number of additional deaths in the Philippines by considering factors such as the current percentage of unvaccinated populations, the number of susceptible people, the maximum outbreak size, and the effectiveness and cost of vaccines. The authors also accounted for the population density and specific interventions like social distancing by incorporating a scaling contact coefficient into the model, which computes the rate of contact based on the population density. The developed model ensured that priority groups, which were selected to be the front-line health workers and old people, were all given priority to receive the vaccines. Furthermore, a model that prioritized groups based on their occupations and age was developed in a study by Babus, Das, and Lee (2020) [23]. The model assumed different scenarios where a stay-at-home order was effective and where there was no order. The policy minimized both the number of deaths and the loss due to the suspension

of the economic activities carried out by those occupations. Their findings suggested that age is more important than occupation.

The authors of [24] developed a multi-period decision-making model to design an allocation strategy by incorporating susceptibility rate and exposure risk while also taking into account operational costs like transshipment between medical centers, capacity, and return mechanism. Their results suggested that superior performance can be achieved in minimizing the risk of susceptibility and integrating the operational costs aspects. However, unlike these studies, this thesis incorporates other factors such as travel time and distance costs, as well as vulnerability indices into the optimization process of costs and allocations.

In the context of forecasting and predicting the death outcomes of pandemics, the author of [25] presented a predictive model named DELPHI-V-OPT that forecasts the number of detected cases, hospitalizations, and deaths for each US state. This model also dynamically captures the effects of vaccination on the pandemic in the sense that vaccinated individuals will be immune to the virus and that reducing the infections will lead to a slower spread of the disease. The model then optimizes the vaccine allocation using the epidemiological data of each state as well as clinical data and availability of the vaccine data to minimize the number of deaths. The output of the model suggested that a decrease of 10 to 25% in the death toll could be achieved, which could save up to 20,000 deaths over a period of three months in the United States. Moreover, authors of [26] formulated a quadratic program that minimizes the sum of quadratic errors between the reported cumulative number of deaths and the predicted number. The model is then formulated into a global optimization problem that is solved using particle swarm optimization to find the parameters that lead to the minimization of the quadratic programming model. The output of the model is then tested in two scenarios, and the results turned out to be fairly close to prior estimates in the

literature. Furthermore, reference [27] discussed the uncertainty associated with the real-time predictions of COVID-19 infection rates, where the authors utilized statistical modeling techniques to predict the spread of the virus in China and Italy. They used a framework to estimate uncertainty as more information becomes available. They noticed that there is an observed shift from exponential growth at the beginning of the pandemic to a sigmoid pattern once lockdown restriction measures are introduced, indicating the effective impact of these measures on the spread of the disease. These studies provide inspiration for how the model could include other important objectives such as reducing deaths from COVID-19.

Finally, reference [28] studied the optimization of the vaccine, where the authors proposed four models to optimize the allocation: minimizing the travel distance and maximizing the vaccination of high-priority groups. The models are developed using a Constraint Satisfaction Problem (CSP) formulation, which is a powerful mechanism to address the logistics of resource allocations. Their four models were: (1) a basic vaccine distribution model, (2) a priority-based distribution model, (3) a distance-based distribution model, and (4) a combination of priority and distance distribution models. They concluded that the last model of the four achieved the best results.

In summary, the fields of vaccine distribution centers optimization and allocation of vaccines have seen significant attention in the past years, particularly in the context of COVID-19. In terms of optimizing the locations of vaccine centers, studies aimed to ensure that the selected sites are in areas that are easily accessible to the populations in general and priority groups in particular. They achieved this by considering factors such as geographical distribution, travel time metrics, and the use of existing retail locations such as dollar stores. The allocation of vaccines has also been a focus of research. Studies have used various optimization techniques along with factors such as

the vulnerability of different groups, fairness, and equity to achieve the most effective allocation plans that minimize the spread of the virus and reduce the number of cases and deaths.

Building on these foundations, this thesis introduces several novel aspects to the field. Firstly, it covers a large metropolitan area, a study area that only a few papers have explored, with an emphasis on the early stages of the pandemic when the number of sites was limited. Secondly, my optimization model considers accurate values of travel times by car and transit and travel distance between the proposed optimal locations and the population centroids of the zip codes of a large metropolitan area. This enhanced accuracy was achieved by using Bing Maps API. The costs associated with those travel times and distances were also incorporated in the model as the objective to be minimized. Lastly, multiple prioritization assignment methods within zones were considered, such as the Healthy Places Index, a vulnerability index based on CDC data, and population-based prioritization. These methods allow exploring different scenarios and their results, providing a more comprehensive study.

Chapter Three: Methodology

The designed optimization model in this thesis is a Mixed Integer Programming (MIP) model that aims to find the optimal locations of vaccine centers and their associated costs in a large metropolitan area. The model assumes that each zip code in the studied area represents a potential site for COVID-19 vaccines and represents a population that needs to be served by these sites. Therefore, the model depends on specific types of data for its computations, such as the actual travel times and distances data between zip codes, the demographics of zip codes, and COVID-19 related data.

3.1 Travel Time and Distance.

Travel times by car and transit, along with the distance matrices, play a significant role in the optimization model and the selection of vaccination sites, as they determined the accessibility of all parts of large metropolitan areas and their residents. To generate the travel times and distances, N by N matrices are created for the travel time by car, travel time by transit, and the distance between the weighted population centroids, where N represents the number of areas/districts/ zip codes in a large city. Each area N in the study serves as a potential site and demand point for the vaccines. These matrices can be obtained in several methods using available software and APIs, each having its advantages and disadvantage for this study. Bing Maps API was selected for the calculations of those matrices due to its accessibility, ease of use, integration with Excel, and accurate results. Excel is utilized in the process where a database with all coordinates were organized. Three new Excel functions are developed using Excel Visual Basic macros, where Excel is connected with the Bing API to generate the results. The matrices can then be computed where the rows are considered as the source points and the columns as destinations, with every cell representing a pair of both. Every cell in the matrix represented the value of either the travel

time in minutes or distance in miles according to the formula generated by Excel macros. The following is a snapshot of a car travel time matrix.

	90029	90280	90031	....
90029	0	25	15	....
90280	26	0	22	....
90031	15	21	0	....
....	....	....	....	0

Table 1: Car travel time matrix in minutes

3.2 Optimization Model.

The optimization model is designed to select the most effective vaccination sites and provide an allocation plan for any major metropolitan city around the globe. The model incorporates a priority assignment parameter that provides the option to assign importance levels to the zip codes based on chosen criteria. In this thesis, the developed model is specifically applied to Los Angeles County, taking into account its diverse demographics and socioeconomic factors. To evaluate the model's robustness and understand how the outcomes vary under different circumstances, we implement three unique scenarios. These scenarios are differentiated based on the following prioritization parameters: using population, the HPI, and a specially developed COVID-19 vulnerability index. The developed MIP model allows both continuous and integer decision variables and relies on solid and robust data sources, which will provide the necessary inputs for a comprehensive study that fits LA County's needs and constraints. The model utilizes travel times by car and transit and the distance between the zip codes in order to find the optimal selection of sites. The objective of the model is to minimize the total costs, which include the cost of opening vaccination sites, the time cost of travel, the distance cost, and the bus cost for those who do not own cars. Additionally, the model aims to maximize the total quantity of vaccines allocated to each zip code based on its priority assignment. The model introduces several constraints to ensure

a feasible and practical solution. It sets the maximum and minimum number of sites to specific numbers, which can be set by decision-makers according to the specifications of each study area. the model also introduces a parameter, denoted as F, which represents the number of vaccine centers people can choose from when receiving their vaccine. This parameter can be adjusted to provide people with more flexibility and convenience. The model also assumes a restriction on the budget, which the cost of opening sites cannot exceed.

3.2.1 Model Sets, Parameters, and Decision Variables.

Sets:

T: Set of time periods t

A: Set of all zip codes areas i

S: Set of all potential sites j

Parameters:

TB_{ij} : Travel time by transit between area i and site j

TC_{ij} : Travel time by car between area i and site j

DD_{ij} : Distance between area i and site j.

O_i : Percentage of car ownership at area i

W_i : Priority assigned for area i.

P_i : Population of area i.

K : Available Budget for opening sites.

Q_t : Available quantity of the vaccine at time t.

TP : Total population of LA county

C : the cost of opening a site.

F : A flexibility parameter indicating the maximum number of sites that people can select from.

M : Big M.

MS : the maximum number of allowable sites.

LS : the minimum number of allowable sites.

VT : the cost value of time.

VD: the cost of traveled distance.

VB: the cost of a public transit ticket.

Decision Variables:

D_i : 1 if area i is selected as a site, 0 otherwise.

X_{ij} : 1 if area i is assigned to site j, 0 otherwise.

V_{ijt} : Allocated vaccines from site j to area i at time t

3.2.2 Objective Function and Constraints

The following objective function is formulated in order to achieve the goal of minimizing the overall costs of administering the vaccines from the selected sites as well as to provide a plan for allocations of vaccines between areas.

$$Min \sum_{j}^{S} D_{\mathrm{j}}\mathrm{C} + \sum_{i}^{A}\sum_{j}^{S}\left(\frac{1}{F} X_{ij} P_i (O_i TC_{ij} + (1 - O_i)\, TB_{ij}) \times 2 \times \mathrm{VT}\right)$$

$$+ \sum_{i}^{A}\sum_{j}^{S}\left(\frac{1}{F} X_{ij} P_i DD_{ij}\, O_i \times 2 \times \mathrm{VD}\right) + \sum_{i}^{A}\sum_{j}^{S}\left(\frac{1}{F} X_{ij} P_i\, (1 - O_i) \times \mathrm{VB}\right) \quad (1a)$$

Subject to:

$$\sum_{j}^{S} V_{ijt} = \frac{P_i}{TP} \times Q_t \quad \text{, for i}\in\text{A, t}\in\text{T} \tag{2a}$$

$$\sum_{j}^{S} D_j \leq MS \tag{3}$$

$$\sum_{j}^{S} D_j \geq LS \tag{4}$$

$$\sum_{j}^{S} X_{ij} \geq F \quad \text{, for i}\in\text{A} \tag{5}$$

$$X_{ij} \leq D_j \quad \text{, for i}\in\text{A, j}\in\text{S} \tag{6}$$

$$\sum_{j}^{S} D_j\, C \leq K \tag{7}$$

$$V_{ijt} \leq X_{ij} M \quad \text{, for i}\in\text{A, j}\in\text{S, t}\in\text{T} \tag{8}$$

$$D_j \geq 0 \quad \text{, for j}\in\text{S} \tag{9}$$

$$X_{ij} = \{0,1\} \quad \text{, for i}\in\text{A, j}\in\text{S} \tag{10}$$

$$V_{ijt} \geq 0 \quad \text{, for i}\in\text{A, j}\in\text{S, t}\in\text{T.} \tag{11}$$

The objective function **(1a)** minimizes the total cost that results from opening the sites, cost of travel time to the vaccination sites, cost of miles traveled, and the cost of bus tickets as follows:

- The first term in the objective function $\left(\sum_{j}^{S} \boldsymbol{D_j C}\right)$, calculates the direct cost resulted from opening the sites.
- The second term of the function $\left(\sum_{\mathbf{i}}^{\mathbf{A}} \sum_{\mathbf{j}}^{\mathbf{S}} \left(\frac{\mathbf{1}}{\mathbf{F}} \mathbf{X_{ij} P_i} \left(\mathbf{O_i TC_{ij}} + \left(\mathbf{1} - \mathbf{O_i}\right) \mathbf{TB_{ij}}\right) \times \mathbf{2} \times \mathbf{VT}\right)\right)$, calculates the cost of time spent by the populations traveling to their F closest sites when they

are given the option to choose from F locations. F is added here to simulate real-life scenarios where the individuals have flexibility in choosing their preferred location to receive the vaccine. Means of travel are accounted for by multiplying the percentage of people who own cars by the TC_{ij} and by multiplying the remaining percentage, which will have to use public transit, by TB_{ij}. The whole term is then multiplied by 2 to account for the round trips and by the travel time cost VT. The whole term is divided by F to account for the average of the F possible trips that could be made by the population, as only one trip is going to take place.

- The term $\mathbf{(\sum_i^A \sum_j^S (\frac{1}{F} X_{ij} P_i DD_{ij} O_i \times 2 \times VD))}$, finds the mile costs of the distance traveled by car users. It is multiplied by 2 to account for the round trip and by VD, which is the cost per mile.
- The fourth term $\mathbf{(\sum_i^A \sum_j^S (\frac{1}{F} X_{ij} P_i (1 - O_i) \times VB))}$, finds the total cost spent by transit users by multiplying the number of trips by the cost of transit ticket VB.

Constraint **(2a)** provides an allocation strategy that is based on the ratio of the population of area i to the total population in all areas multiplied by the available vaccine quantities Q_t for the given period t. Constraint **(3)** sets the maximum allowable sites to MS. Constraint **(4)** sets the minimum possible sites to LS. Constraint **(5)** sets the number of options the populations of each area can have to a minimum of F. Constraint **(6)** is an upper bound constraint to link decision variables X_{ij} and D_j. Constraint **(7)** sets the maximum budget for the costs of opening sites to K, which can be adjusted by policymakers. In constraint **(8)**, the amount of vaccines allocated is linked to the assignment between areas and sites so that vaccines are only allocated when there is an assignment, where M is a large positive number that acts as an upper bound on V_{ijt}. M value could be as low as the amount of vaccines available at t. Constraints **(9)**, **(10)**, and **(11)** regulate the value of the decision variables.

3.3 Modeling The Different Scenarios

In this section, three scenarios will be discussed and applied to the introduced model to provide a more comprehensive analysis of the model from different perspectives. The following scenarios were not intended to represent the best strategies, but rather to demonstrate the model's ability to accommodate different prioritization strategies based on the specific needs and constraints of the given situations and area of study. By doing so, we can gain insights in how different strategies impact the outcomes and effectiveness of the optimization problem, which in return, will provide guidance to decision-makers. The implementation of these scenarios is built on the assumption than comprehensive data and indices about zip codes is readily available for the intended area of study. The feasibility of these scenarios is directly tied to the extent and quality of available data.

3.3.1 Scenario One: Prioritizing Areas Based on Population.

In the first scenario, the population will serve as the weighting factor when deciding on the importance and assigning the priorities of the areas. Therefore, the model in this case, will favor the areas with higher populations and select the sites and allocation plan accordingly.

The objective function and constraints remain the same, as described and explained previously in this chapter.

3.3.2 Scenario Two: Prioritizing Areas Based on the Healthy Places Index.

In scenario two, we utilize the HPI, a comprehensive tool that calculates an overall health score for regions based on multiple factors such as socioeconomic conditions, environmental characteristics, and accessibility to healthcare [29] (more discussion on HPI can be found in section **4.2.2**) . HPI data is used as the weighting factor. We will rank all areas based on their HPI percentile, as provided by The Public Health Alliance of Southern California. Five categories, 1

(most important) thru 5 (least important), are then introduced, and areas are categorized based on their percentile. The population of each area will be multiplied by a multiplier based on the area's category to yield Wi for each area i that will be used in the model, as explained in the following table:

Percentile Range	Category	Weighted Population (Wi)
0.19 - 0	1	population x 1.5
0.39 - 0.2	2	population x 1.25
0.59 - 0.4	3	population x 1
0.79 - 0.6	4	population x 0.75
1 - 0.8	5	population x 0.5

Table 2: Wi calculations using HPI

The new W_i will only change the objective function and the first constraint. The rest of the model will remain unchanged. The modified objective function and constraint are as follows:

$$Min \sum_{j}^{S} D_j \mathrm{C} + \sum_{i}^{A}\sum_{j}^{S}(\frac{1}{F} X_{ij} W_i (O_i TC_{ij} + (1 - O_i)\, TB_{ij}) \times 2 \times \mathrm{VT}) + \sum_{i}^{A}\sum_{j}^{S}(\frac{1}{F} X_{ij} W_i DD_{ij}\, O_i \times 2 \times \mathrm{VD}) + \sum_{i}^{A}\sum_{j}^{S}(\frac{1}{F} X_{ij} W_i\, (1 - O_i) \times \mathrm{VB}) \quad (1b)$$

$$\sum_{j}^{S} V_{ijt} = \frac{W_i}{\sum Wi} \times Q_t \quad \text{, for } i \in A, t \in T \quad (2b)$$

3.3.3 Scenario Three: Prioritizing Areas Based on the Vulnerability to Covid-19.

In this scenario, the weighting factor W_i will be calculated based on how different ethnicities are vulnerable to Covid-19. The following table is provided by the Centers for Disease Control and

Prevention (CDC) [30], and it outlines the risks of getting infection, hospitalized, and death by Covid-19 by race and ethnicity.

Race/Ethnicity	American Indian or Alaska Native, Non-Hispanic	Asian, Non-Hispanic	Black or African American, Non-Hispanic	Hispanic or Latino
Cases	1.6x	0.8x	1.1x	1.5x
Hospitalization	2.4x	0.7x	2.0x	1.8x
Death	2.0x	0.7x	1.6x	1.7x

Table 3: Racial vulnerability to Covid-19 by CDC

The "x" in these values shows the rate ratios compared to White, Non-Hispanic race. For instance, a Black Non-Hispanic individual is 1.1 times more likely to get infected, two times more likely to get hospitalized, and 1.6 times more likely to die from the virus compared to a White individual. These rates, combined with the racial compositions for the targeted areas of study, are used for the calculation of the Covid-19 racial vulnerability index. A weighted score for each of the three risks (cases, hospitalization, death) measures is computed by multiplying the rates from the above table by the proportion of each race for each area. The output of the above calculations will result in a score for each of the above three risk measures. The following table is an example of these calculations for an area for demonstration:

Race	Population	% of Total Population	Risk Ratio (Cases)	Weighted Cases Risk	Risk Ratio (Hospitalization)	Weighted Hospitalization Risk	Risk Ratio (Death)	Weighted Death Risk
American Indian and Alaska Native, Non-Hispanic	88	0.0025	1.6	0.004	2.4	0.006	2	0.005
Asian, Non-Hispanic	5471	0.1546	0.8	0.1237	0.7	0.1082	0.7	0.1082
Black or African American, Non-Hispanic	1301	0.0368	1.1	0.0405	2	0.0736	1.6	0.0589
Hispanic or Latino	19899	0.5623	1.5	0.8435	1.8	1.0114	1.7	0.9559
White only	8629	0.2438	1.0	0.2438	1.0	0.2438	1.0	0.2438
Total / Composite Risk Score	35488	1	-	**1.2555**	-	**1.443**	-	**1.3618**

Table 4: Risks scores calculations example for zip code 90029

Following the above calculations, we combine all three risk scores into a single score for all three by assigning a weighting factor for each of the risk measures. We assigned a weight of 0.15, 0.3, and 0.55 to cases, hospitalization, and death, respectively as shown in the following table:

Risk Measure	Weight
Cases	0.15
Hospitalization	0.3
Death	0.55

Table 5: Weights for risks measures

The selection of these weights is subjective and was chosen based on the severity of the risks, with death being the most serious risk. Finally, by implementing the previous steps in all areas of study, we end up with a final score for each. The percentiles are calculated for all areas, and then the areas are categorized into five categories, similar to the earlier categorization method used in scenario two. Each percentile is multiplied by a multiplier based on the category to yield W_i, which will be reflected on the objective function and the first constraint as described before.

Chapter Four: Study Area and Datasets

4.1 Los Angeles County Metropolitan Area.

Los Angeles County is the most populous County in the United States, with an estimated population of over 10 million residents of mixed and diverse ethnicities and backgrounds. The County is composed of a varied mix of urban, suburban, and rural areas, offering a comprehensive view of various community settings, from the Pacific Ocean in the west to the San Gabriel Mountains in the east, which could pose challenges and impact the distribution and administration process of the vaccines. The demographic composition of LA County is extremely diverse. According to the US Census Bureau [31], the County consists of 49% Latinos, 25.5% White, 7.6% Black, 14% Asians, and less than 1% American Indian and Alaska Native. The County is also linguistically diverse, with many distinct languages spoken in households, with the English and Spanish being the most common ones. In addition, socioeconomic factors, such as income level, education, occupations, and accessibility to cars, widely range in the area which could eventually lead to health outcome disparities. Moreover, Los Angeles County consists of around 295 zip codes, of which 277 are considered for the scope of the thesis after excluding some of the incorporated areas in the County due to the lack of sufficient data needed to conduct the study. Catalina Island zip codes were also excluded because they are accessible only by ferries and airplanes. Each zip code has its own unique demographics and geographic characteristics, which will result in more informed, tailored, and effective vaccine distribution centers and allocations. The following map shows the populations of the zip codes in LA County:

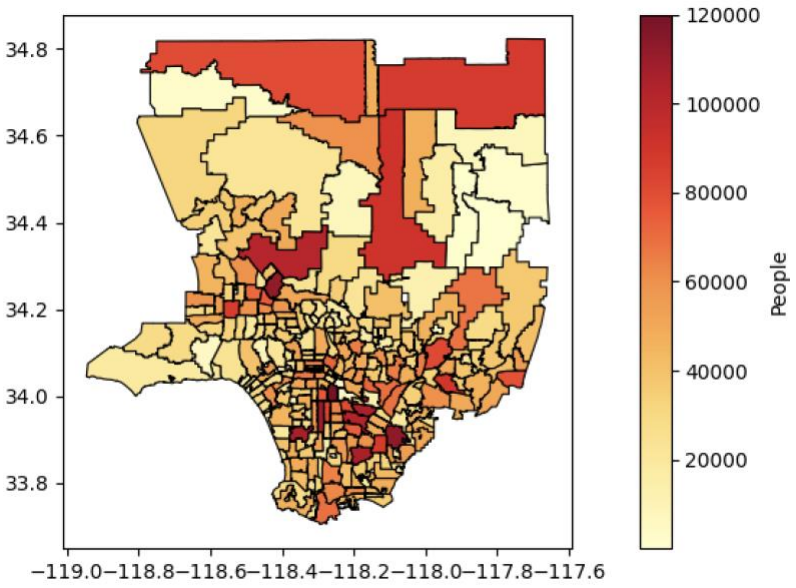

Map 1: LA County population heatmap

The application within this thesis covers 12 biweekly periods (approximately five months and a half) starting from the day the first vaccine was approved by the Food and Drug Administration (FDA) on 12/14/2020 and continuing until 05/30/202. This timeframe was chosen to focus on the initial phase of the pandemic when the sites and vaccine availability were limited.

A 277 by 277 matrices were generated by Bing Maps for car travel time, transit travel time, and distance between the zip codes. Random values were chosen and compared with actual times, and all were within 10% margin of error.

The parameter F in the model is assumed to be 3, this is to ensure people are given more than one option and to simulate real-life flexibility. The value of parameter VT for LA County is set at $0.264167. This number represents 50% of the average wage per minute in the County. According to the US Department of Transportation [32], 50% is the recommended percent of wages for the travel time valuation when the trip purpose is personal. The value of parameter VD is $0.615, which is the suggested cost per mile in Southern California as per the American Automobile

Association [33]. Parameter VB represents the cost of public transit tickets, which is approximately $1.75. The values of parameters C and K, which represent the cost of opening a site and the total available budget, are assumed to be $500,000 and $10 million, respectively. These numbers are hypothetical and were chosen to provide a framework for the model. Actual costs that are based on real-life data on the availability of budgets should be used in the application of the model.

4.2 Datasets

The selection and use of appropriate datasets are crucial in carrying out an effective study. Several large datasets were utilized in this thesis to enhance and inform the process of optimally locating the vaccination sites and the quantity allocated to each one.

4.2.1 Demographic Data

Demographic data was taken from the U.S. Census Bureau [29] and utilized throughout the thesis. It provides a complete breakdown of the racial and age groups composition of the County on the zip code level. This level of detail is essential in order to make tailored and informed decisions and outcomes.

4.2.2 Healthy Places Index

The Healthy Places Index (HPI), as described by [34], is a tool that provides data on numerous elements that influence the areas' health. It calculates an overall health score for regions using a variety of factors, such as socioeconomic factors, environmental characteristics, neighborhood conditions, healthcare accessibility, and more. The HPI is computed by standardizing 25 indicators across 8 domains, calculating domain scores, and weighting them using a regression model against life expectancy. The final score for each zip code is then calculated and validated to inform decisions about the communities' health. The scores are ranked from 1 to 99, with higher scores

indicating better healthy areas. This index was developed by The Public Health Alliance of Southern California [29] for multiple counties within the state of California. This index provides a powerful tool that could be used by policymakers in various fields and help them make more informed decisions. The HPI will be utilized in this thesis to analyze different scenarios of the optimization model.

4.2.3 Covid-19 Data

Data on the quantity of vaccines administered is sourced from the LA County Department of Public Health [35]. It also displays the number of vaccines and the date of when they were delivered and administered to each neighborhood within the LA county, which will serve as the assumed available quantities in this thesis.

4.2.4 Vulnerability to Covid-19

In order to simulate different scenarios and analyze how the output behave, we will be introducing a COVID-19 vulnerability index that takes into calculations the data provided by the Center for Disease Control and Prevention (CDC) [30] on how certain racial groups are vulnerable to get infected, hospitalized, and potentially die from the virus. This, when paired with the demographics of each zip code, provides insights and helps design a better and more strategic solution.

4.2.5 Car Ownership Data

In order to capture more accurate results when it comes to the calculations of the travel times and the trips made by the population of each unit of study (zip codes), the number of households owning a car is needed and is sourced from the 5-Year American Community Survey Data provided by the U.S Census Bureau [36]. This data consists of several house characteristics that will help in estimating how many people in each zip code would use public transportation or their

private cars to travel to vaccination sites. For this thesis, we are interested in the percentage of households owning at least one car.

4.2.6 Geographical Data

LA County shapefiles and geographical data will be utilized in this thesis to develop different types of maps, which help analyze and visualize the areas of the County. These data were sourced from the Los Angeles GeoHub [37]. Moreover, Travel times by both bus and cars, as well as the distance between the zip codes in LA County, were generated using Bing API. Furthermore, the zip codes' population-weighted centroid coordinates were retrieved from the Office of Police Development and Research and then were utilized as potential facilities for the administration of the vaccines. They were used during the computations of the travel times and distances matrices as well.

Chapter Five: Results and Discussion.

In this chapter, we look at the results of applying our optimization model to the three defined scenarios, where we focus on the total costs, selection of the vaccine distribution centers, and the allocations plan of the limited vaccine quantities, and then a sensitivity analysis will be conducted to examine the robustness of our results.

5.1 Model Output for Optimal Vaccine Distribution Sites.

5.1.1 Scenario One:

The optimal objective value for the first scenario is Z= $194,815,903. The following table showcases the breakdown of the costs:

Cost Type	Cost ($)
Construction Cost	10,000,000.00
Travel Time Cost	89,647,526.18
Travel Distance Cost	93,682,480.82
Bus Ticket Cost	1,485,895.97
Total	194,815,902.98

Table 6: Optimal costs breakdown

As shown in the table, the travel time and distance costs contribute the most to the overall costs since the number of trips to be made is very large. Moreover, the following LA map shows the selected optimal sites when the population is the weighting factor.

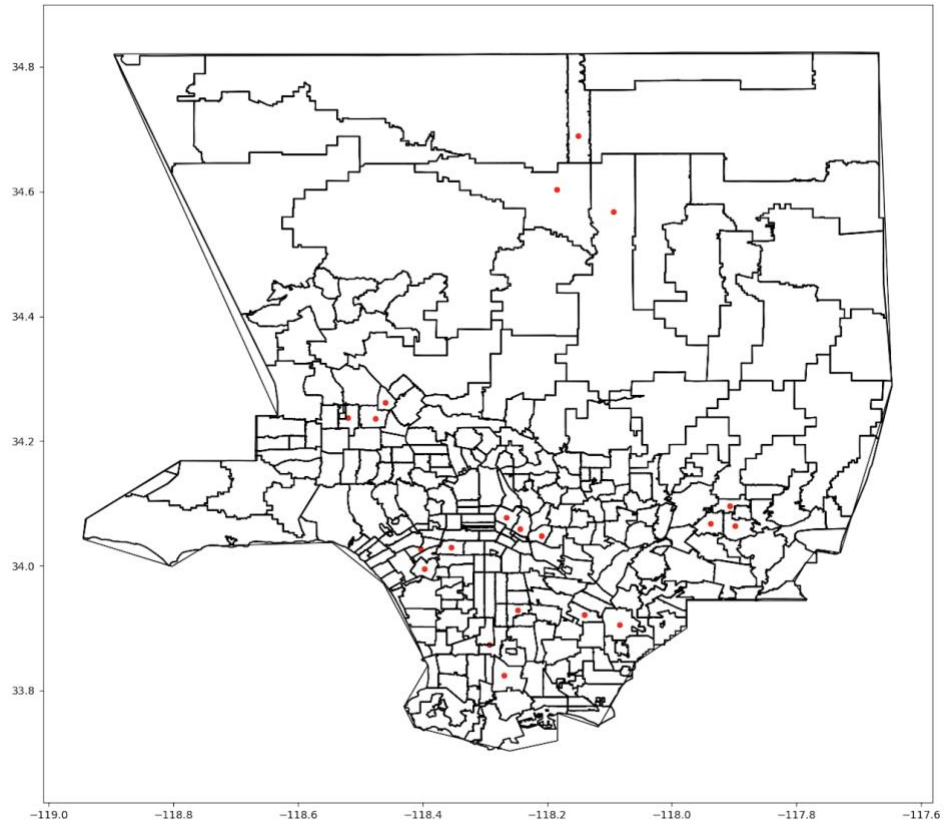

Map 2: Map of optimal sites for the first scenario

The following scatterplots show the relationship between the average travel times for bus and cars as well as the average traveled distance with the populations of the areas.

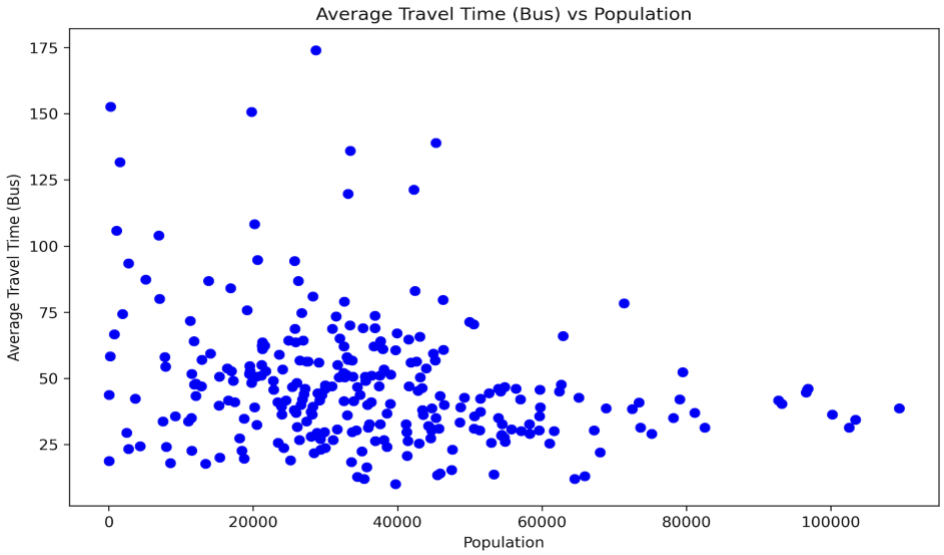

Figure 2: Scatterplot of average travel time by transit vs population of zip codes

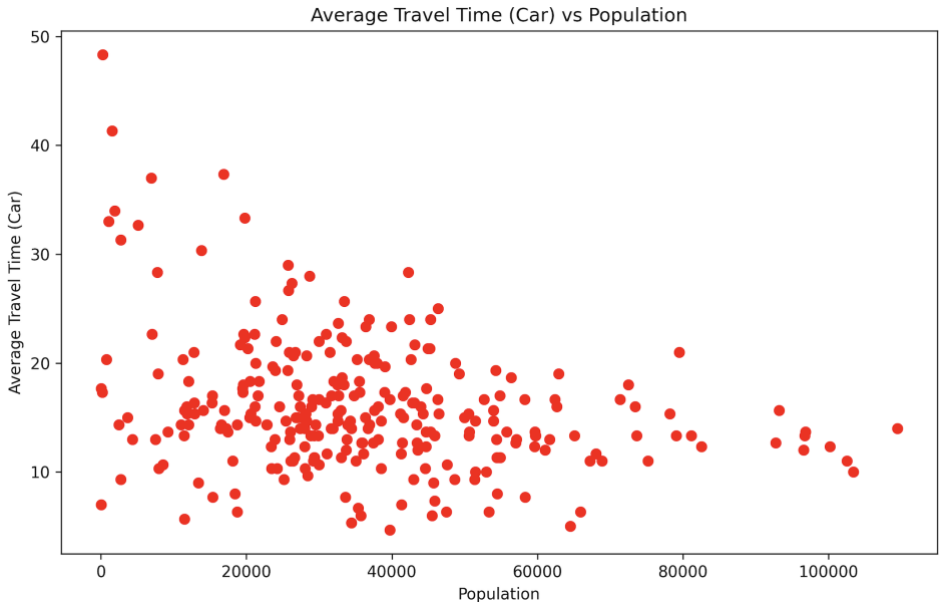

Figure 3: Scatterplot of average travel time by car vs the population of zip codes

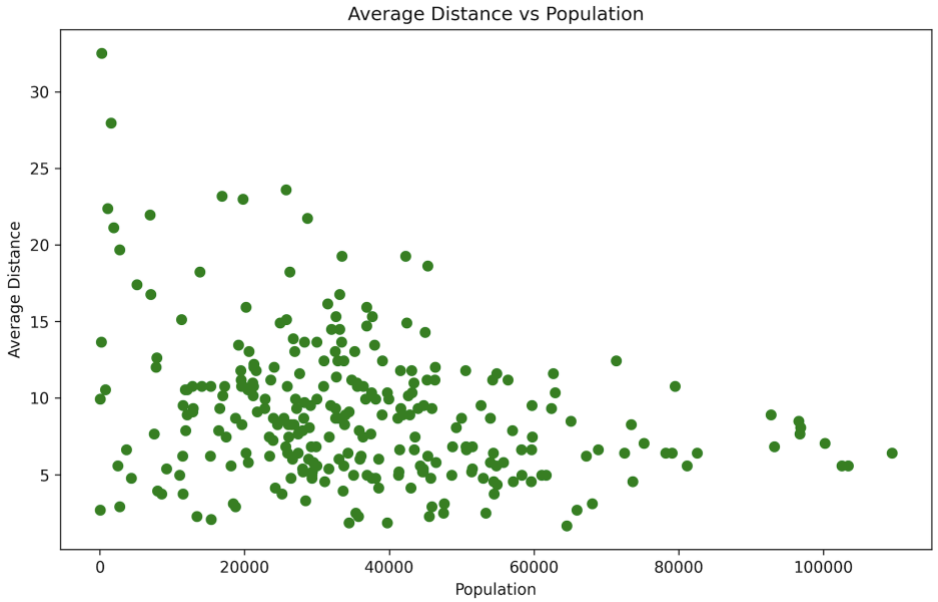

Figure 4: Scatterplot of average distance vs the population of zip codes

As shown in the previous charts, the relationship between the populations and the average travel and distance is inversely proportional, which is reasonable considering that this scenario aims to prioritize more populated areas.

5.1.2 Scenario Two:

The optimal objective value when applying the second scenario on the model is Z = $204,038,094.2, and the following table shows the breakdown of the costs:

Cost Type	Cost ($)
Construction Cost	10,000,000.00
Travel Time Cost	90,351,438.72
Travel Distance Cost	94,565,654.05
Bus Ticket Cost	1,485,895.97
Total	196,402,988.73

Table 7: Optimal costs breakdown for scenario 2

Please note that Z is different from the total costs since the costs are calculated based on the true populations making the trips without Wi affecting the actual costs. The following is the map of the selected sites:

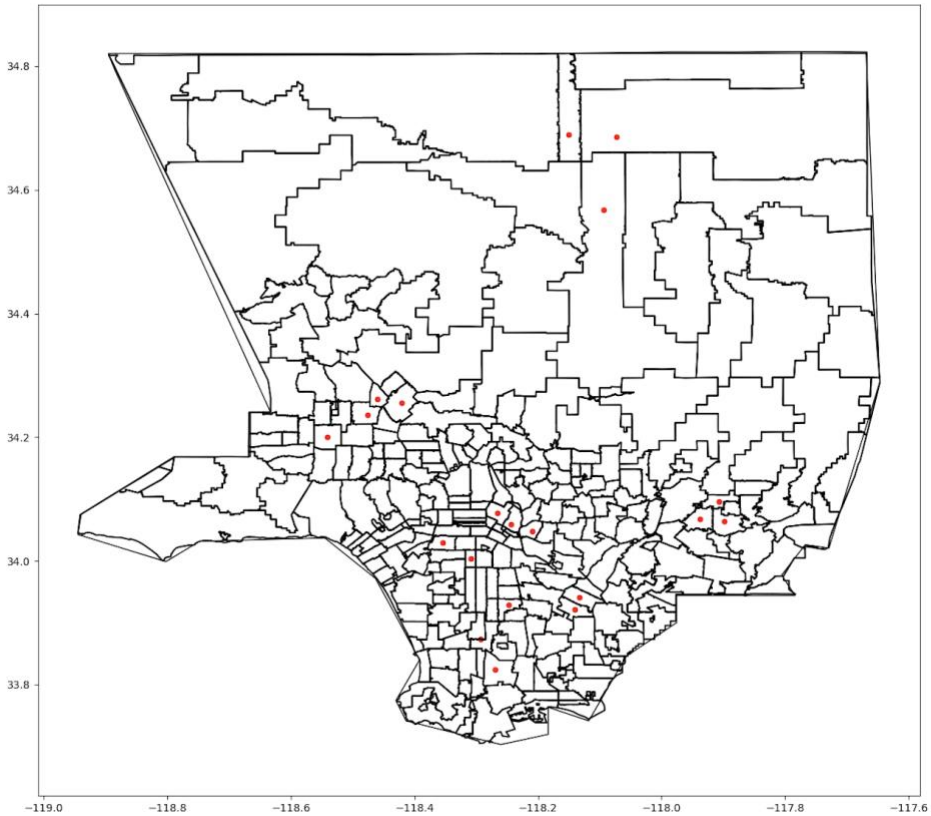

Map 3: Map of optimal sites for the second scenario

Figure 5 shows the box plot of the HPI percentile for the selected sites and compares it to the non-selected sites. As expected, the plot shows a notable difference in the median of the selected sites vs the non-selected, where the sites appear to be in zip codes within the lower side of percentiles.

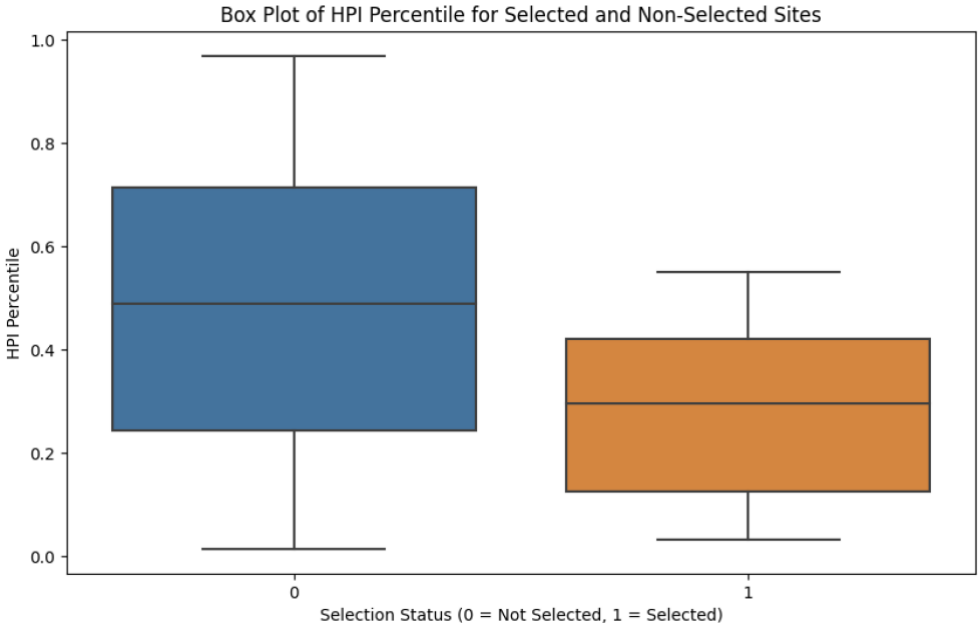

Figure 5: Box plot of HPI percentile for selected sites

5.1.3 Scenario Three:

When applying the third scenario with the developed Covid-19 vulnerability index, the optimal objective becomes Z = $182,327,956.5, and the following table shows the breakdown of the costs:

Cost Type	Cost ($)
Construction Cost	10,000,000.00
Travel Time Cost	92,633,900.93
Travel Distance Cost	95,914,698.13
Bus Ticket Cost	1,485,895.97
Total	200,034,495.03

Table 8: Optimal costs breakdown for scenario 3

Please note that Z is different from the total costs since the costs are calculated based on the true populations making the trips without Wi affecting the actual costs. The following is the map of the selected sites:

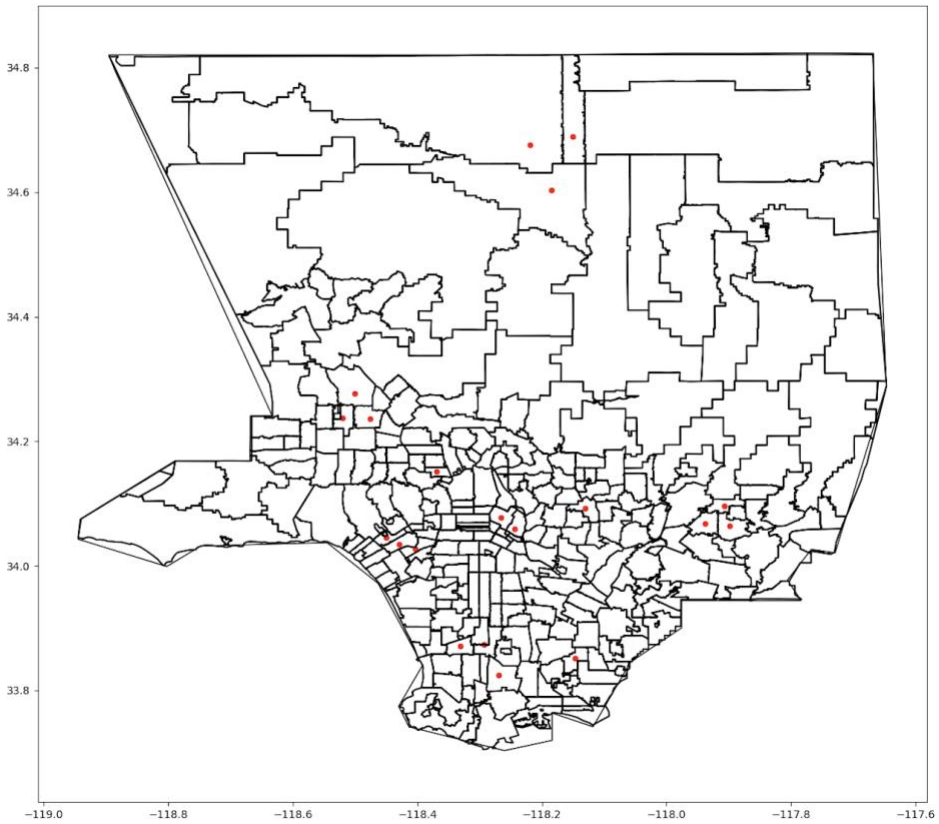

Map 4: Map of optimal sites for third scenario

The following table summarizes the travel time cost, distance cost, and total weighted cost for all scenarios:

	Cost type		
Scenario	Travel time cost ($)	Distance cost ($)	Total weighted cost ($)
1	89,647,526.18	93,682,480.82	194,815,902.98
2	90,351,438.72	94,565,654.05	196,402,988.73
3	92,633,900.93	95,914,698.13	200,034,495.03

Table 9: Summary of cost types for all scenarios

In scenario 1, the total weighted cost, which includes both the travel time and distance cost as well as cost of opening sites and the bus ticket costs, is approximately $194.8 million. The second

scenario yielded a higher total weighted cost of around $196.4 million, which is due to the increase of both the travel time cost and distance cost from the first scenario. In scenario 3, we observe a further increase to approximately $200 million, which is also a result of the travel time and distance increase. These results highlight the trade-offs involved in the optimization model. Different prioritization techniques will result in different objective functions but could also mean better public health outcomes.

5.2 Model Output Optimal Vaccine Distribution Sites:

5.2.1 Scenario One:

The following heatmap demonstrates the allocation quantities to all selected areas, which will then be serving all zip codes around them based on the assignment output of the model.

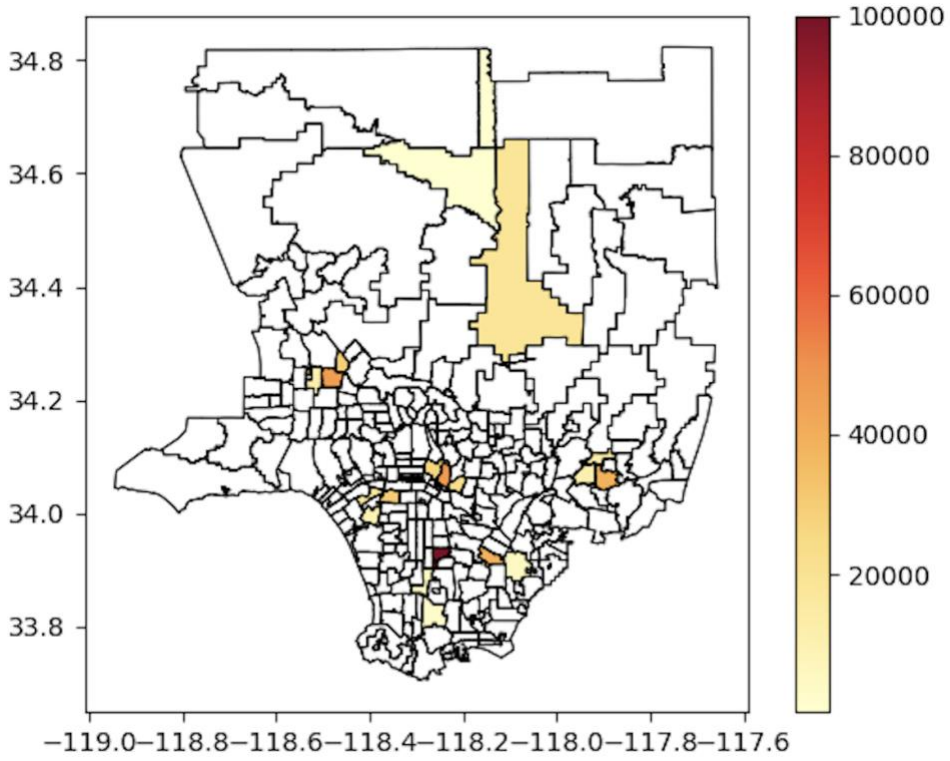

Map 5: Vaccine allocation for the first scenario

As can be observed from the above map, most of the vaccine quantities are allocated towards and near the areas where the population is very high (map 1 shows the population for reference).

5.2.2 Scenario Two:

The following heatmap demonstrates the allocation quantities to all selected areas when the second scenario is applied, which will then be serving all zip codes around them based on the assignment output of the model:

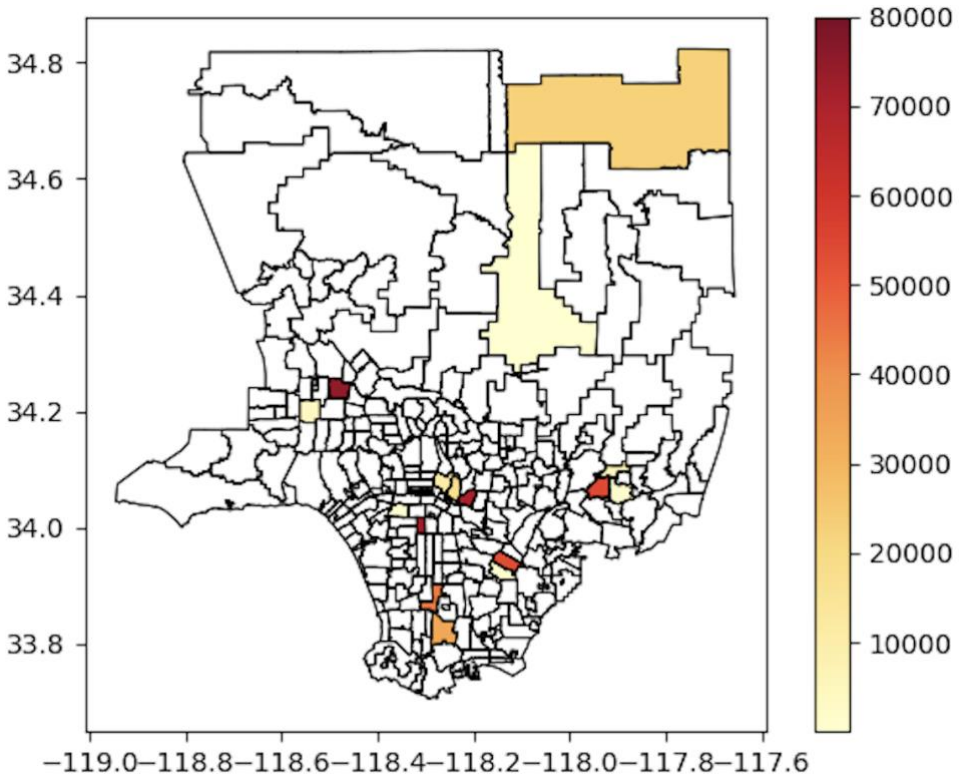

Map 6: Vaccine allocation for the second scenario

5.2.3 Scenario Three:

The resulted allocations of the vaccines for the third scenario are demonstrated in the following heatmap:

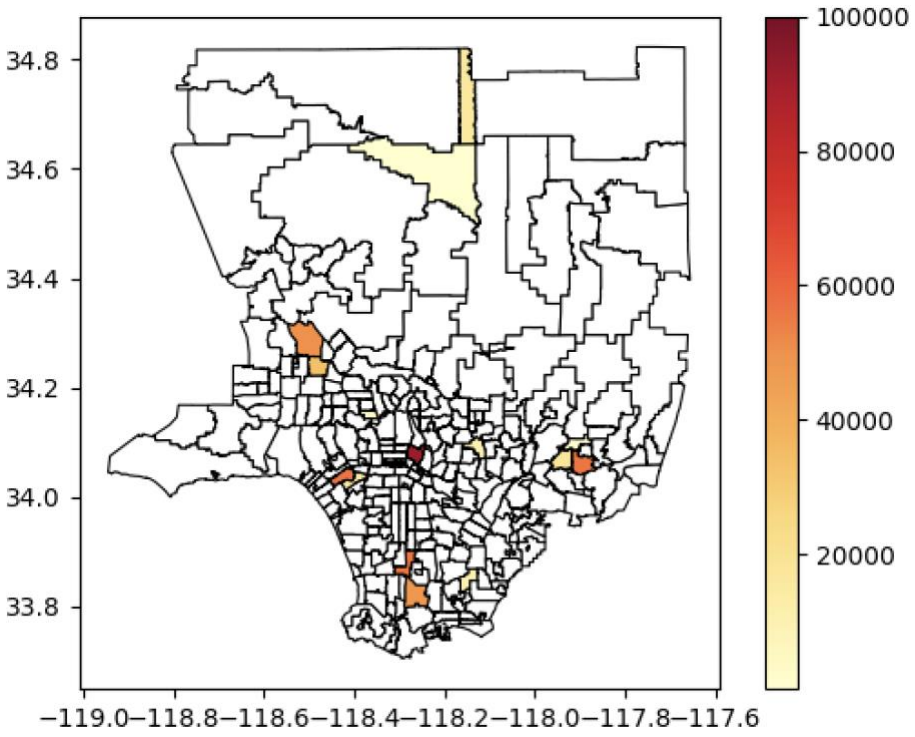

Map 7: Vaccine allocation for the third scenario

The following table shows the average travel times both for cars and transit as well as the average distance for all scenarios:

	Scenario 1	Scenario 2	Scenario 3
Average Travel Time (Bus) (Min)	47.4	48.9	48.5
Average Travel Time (Car) (Min)	16	16.3	16.2
Average Distance (Mile)	9	9.3	9

Table 10: average travel times and distance values for all scenarios

After running the three scenarios, we could observe that the first scenario yielded the least total costs, as well as better average values for times and distances. However, the higher costs and slightly longer times and distances could be traded for the purpose of making the locations more accessible to the people in need the most.

5.3 Sensitivity Analysis.

For sensitivity analysis, two types of analysis are conducted as follows:

- Changing the maximum number of sites between 7 and 40.
- Changing the flexibility for the number of sites people can choose from.

These two are done for the first scenario in this section, and the results for the second and third scenarios can be found in the appendix.

5.3.1 Changing the Maximum Number of Sites.

An important part of the analysis is testing the sensitivity of the model results to changing the maximum number of allowed vaccine distribution sites. This is implemented by changing the range of the number of allowed sites between 7 and 40. The output for all iterations for all three scenarios can be found in the appendix in Table 13 through 15, and it is displayed in the following charts, showcasing the objective function (total costs), breakdowns of the costs, and the average travel times in car and bus as well as the average traveled distance for some of the iterations:

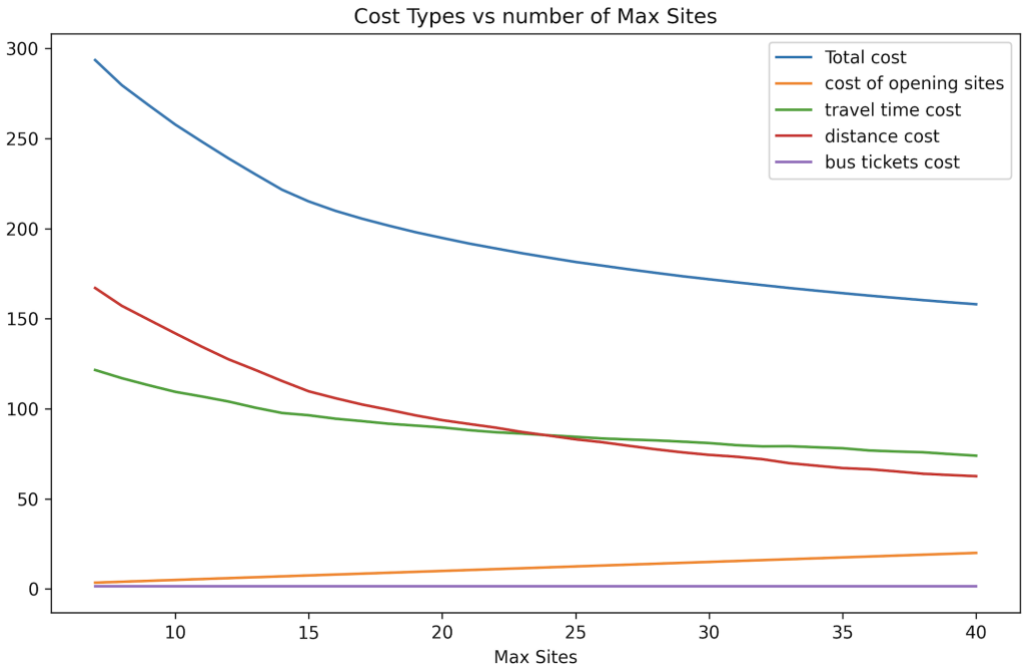

Figure 6: Cost types vs number of maximum sites

As can be observed in Figure 6, starting from a baseline of 7 sites, the total cost decreases as the number of sites increases. The cost of opening sites increases linearly as more sites are added, which is expected since each additional site involves a fixed cost. The bus ticket cost is constant as the number of trips is unchanged and reflects the number of people who do not own cars regardless of the number of sites. The travel time cost and the distance cost decrease as more sites are open, indicating the cost-effectiveness of having more sites that are spread out across the County. The decrease in total cost, as well as the travel time and distance costs, become less significant with each additional vaccination site.

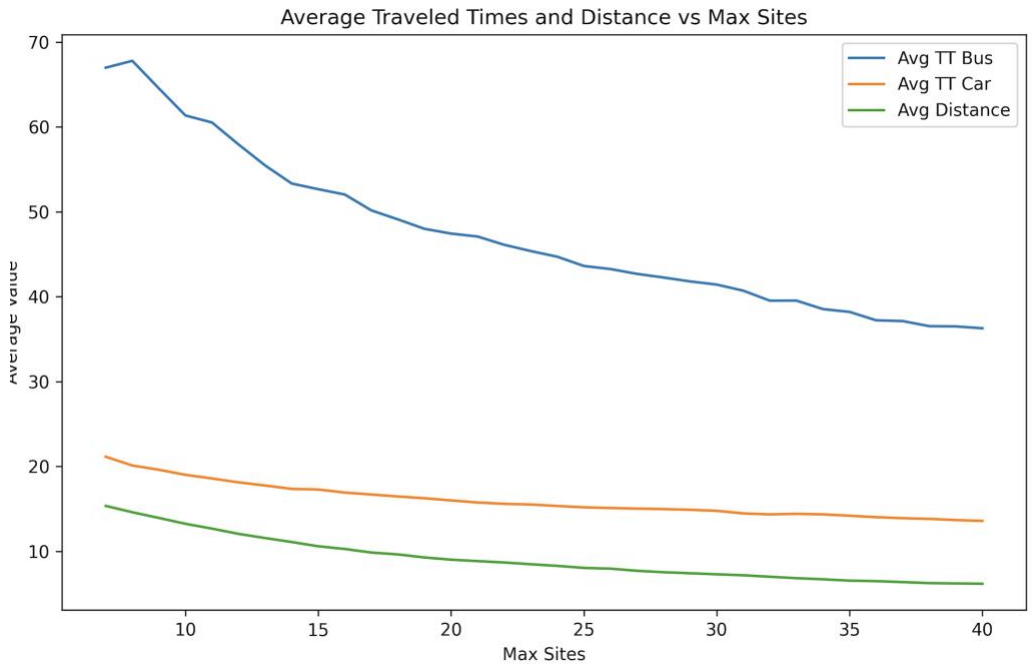

Figure 7: Average travel times and distance vs max sites

Similarly, figure 7 shows a trend of reduction in the average travel time by bus and car and the average distance traveled as the number of sites increases. A significant reduction is observed in the average travel time for bus users, which emphasizes the importance of opening more sites to increase accessibility for people who rely on public transit. A less steep decrease is seen for car users, which is expected since these individuals are generally more mobile and less influenced by

the number of available centers. Overall, the results demonstrate the advantage of having more vaccination sites, showcasing their benefits in terms of time and cost savings for the public. Figures 12 through 15 shows these charts for sensitivity analysis on scenario 2 and scenario 3, which can be found in the appendix.

Table 11 shows a comparison of the total costs for different maximum sites inputs for all scenarios when Pi is the weighting factor for all . As can be observed across all the values of maximum sites, scenario 1 almost always yields the minimum total costs. In reality, prioritization based on population might be the most straightforward approach, which ensures maximum number of people have more access to vaccination centers.

	Total Cost Using Pi as the weghiting factor				
	Maximum Sites Number				
Scenario	7	15	20	25	35
1	293,530,630	215,072,181	194,815,902	181,461,824	164,154,071
2	293,530,631	215,873,640	196,402,989	184,380,838	166,859,124
3	296,432,268	219,795,157	200,034,495	186,274,012	168,092,380

Table 11: Total cost for different max sites for all scenarios

Table 12 shows the same comparison when the HPI is used as the weighting factor for the calculations of the total cost for the solutions. The second scenario in this case always yielded the minimum total costs. In the real-world context, this approach ensures that areas with less healthy measures have more access to the vaccines.

	Total Cost Using HPI as the weghiting factor				
	Maximum Sites Number				
Scenario	7	15	20	25	35
1	314,211,669	224,258,711	206,463,780	192,624,605	175,583,854
2	314,211,669	223,104,384	204,038,094	190,008,979	172,629,281
3	320,952,051	235,975,067	218,327,102	204,744,962	185,368,606

Table 12: Total cost weighted by HPI for different max sites for all scenarios

Table 13 shows the total cost when the COVID-19 vulnerability index is used as the weighting factor when calculating the total cost for the solutions of each scenario. The table below shows that scenario 3 yielded the minimum costs for all different maximum site numbers. This approach would ensure that areas most at risk from the virus are prioritized, which potentially will reduce the spread and impact of the disease.

	Total Cost Using COVID-19 Vulnerqability Index as the weghiting factor				
	Maximum Sites Number				
Scenario	7	15	20	25	35
1	274,597,515	206,453,642	185,640,461	172,862,364	153,968,630
2	274,597,515	208,648,060	190,659,797	179,711,961	161,123,811
3	272,518,937	203,221,875	182,327,957	168,479,526	151,182,940

Table 13: Total cost weighted by COVID-19 Vulnerability Index for different max sites

This sensitivity analysis shows that as the number of sites increases, the total costs decrease, primarily due to the significant contribution of time and distances costs to the overall cost. These outputs underscore the trade-offs involved in selecting different priority assignments when optimizing the vaccine sites, which could justify the less optimal solutions in some instances.

5.3.2 Changing the Number of Sites Residents Can Choose From (F).

The second analysis that is conducted on the model is to change the number of sites each resident can choose from by changing the parameter F in the model. The model is run with F=1 and F=5 to test how this change affects the selection of the sites. In map 8 below, we can see the selected optimal sites when F=1.

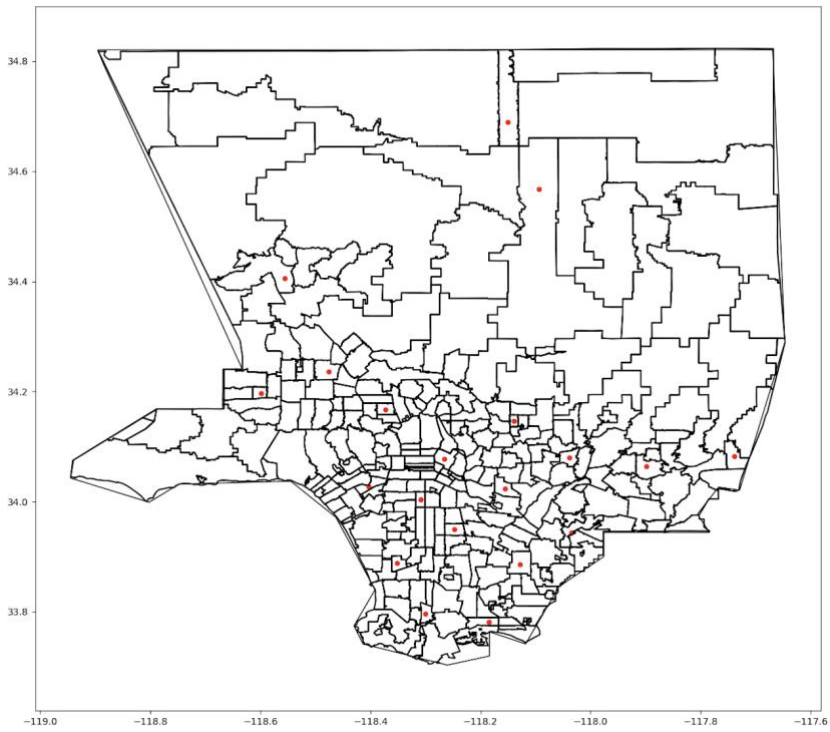

Map 8: Map of optimal sites when F=1

And the following map shows the sites when F=5.

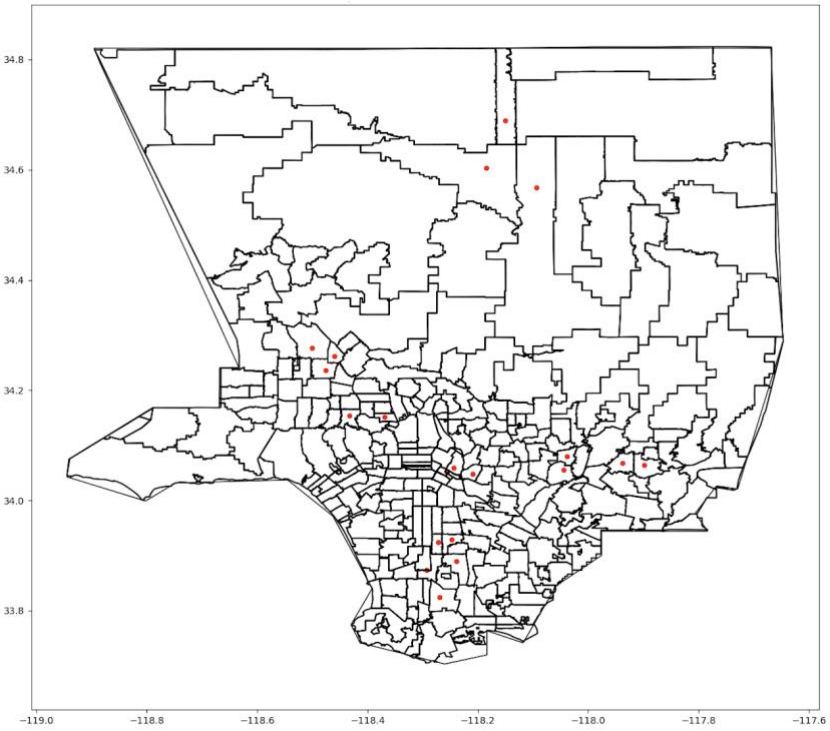

Map 9: Map of optimal sites when F=5

We notice that as the number of options (F) given to the populations increases, the model tends to select sites that are adjacent to each other, and as the number decreases, the selected locations are far spread from each other. This trend could be explained as that the model is trying to select as fewer sites as it could and potentially select a single site if it was possible. Another explanation for this would be that areas with higher populations are more favorable to be near the optimal locations, and therefore the model tends to select the number of sites equal to F it was given, all next to areas that are highly populated.

Similar sensitivity analysis was conducted for scenario 2 and scenario 3, and their resulted maps (Map 11 through 14) can be found in the appendix section.

Table 12 shows the total weighted costs when F is equal to 1, 3, and 5 for all three scenarios.

	Total weighted cost ($)		
	Flexibility parameter (F)		
Scenario	1	3	5
1	122,738,270.51	194,815,903.00	245,332,618.45
2	125,869,410.61	196,402,988.73	248,242,439.57
3	127,534,927.50	200,034,495.03	247,077,458.39

Table 14: Total weighted costs for different F values for all scenarios

As can be observed from the table, the value of the objective function gets worse as the parameter F increases. Providing more choices might be more convenient for individuals, but it comes with a cost. The model incorporates this trade-off by allowing the F value to be adjusted, which helps capture the impact of levels of choice on the overall cost.

5.4 Comparison Between the Optimal Sites vs the Actual LA County Vaccine Sites.

In this section, we will compare the model's optimal costs for the selected sites and then compare it to the actual sites that were operational in Los Angeles County. During the early phase of vaccination, there were 9 locations established to provide the residents of the County with the vaccine, according to NBC Los Angeles [38]. Those locations were:

1. Dignity Health Sports Park in Carson.
2. Cal State LA.
3. Cal Poly Pomona.
4. Dodger Stadium.
5. Pomona Fairplex.
6. The Forum.
7. Cal State Northridge.
8. Los Angeles County Office of Education.
9. Six Flags Magic Mountain.

The following map shows the locations for these 9 sites:

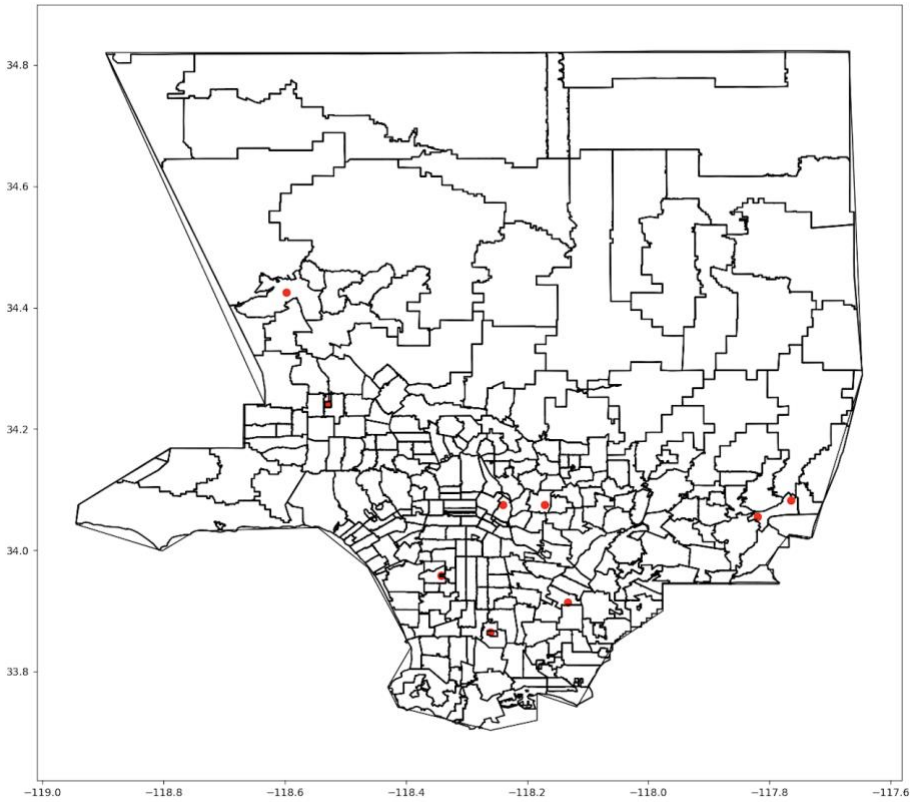

Map 10: Map of the actual vaccine sites in LA county

As can be observed from the map, the distribution sites are scattered across the region. However, some highly populated areas, particularly in the northern and northeastern parts of LA County, appear to be situated at long distances from these sites.

To ensure a fair comparison, the proposed model will be applied with a maximum limit of 9 sites, mirroring the actual number of sites. The model will be executed for both the existing sites as well as the three proposed scenarios, allowing us to compare the output effectively.

- **When F=3:**

The following chart shows the values for the average travel times and distance for all scenarios vs the actual sites, along with the average improvement percentage:

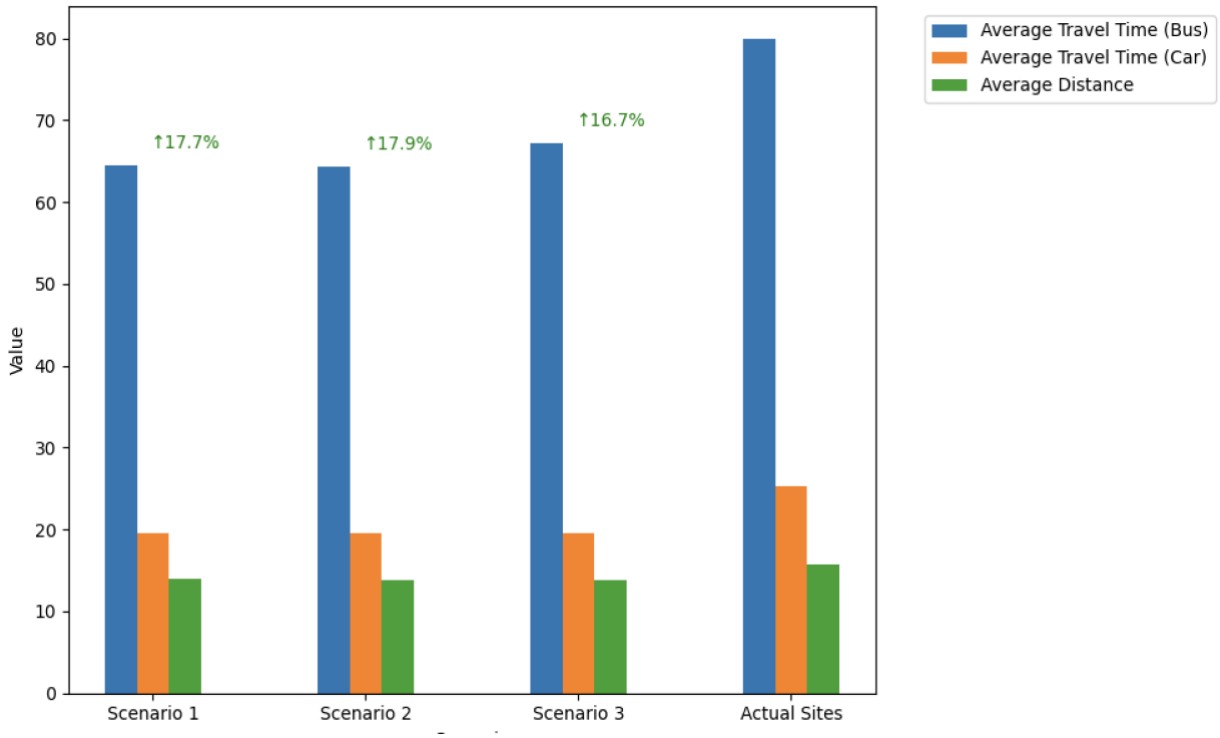

Figure 8: Average travel times and distance comparison

As observed from the chart, we can see that the second scenario resulted in the lowest average times with an average improvement of 17.9% from the actual sites travel times and distance. Similarly, the three scenarios' optimal costs were an improvement from the total cost of the actual sites, with a 17% cost reduction achieved by the first scenario. The following chart shows the total cost and its breakdown for all the scenarios and the actual sites, along with the savings percentage:

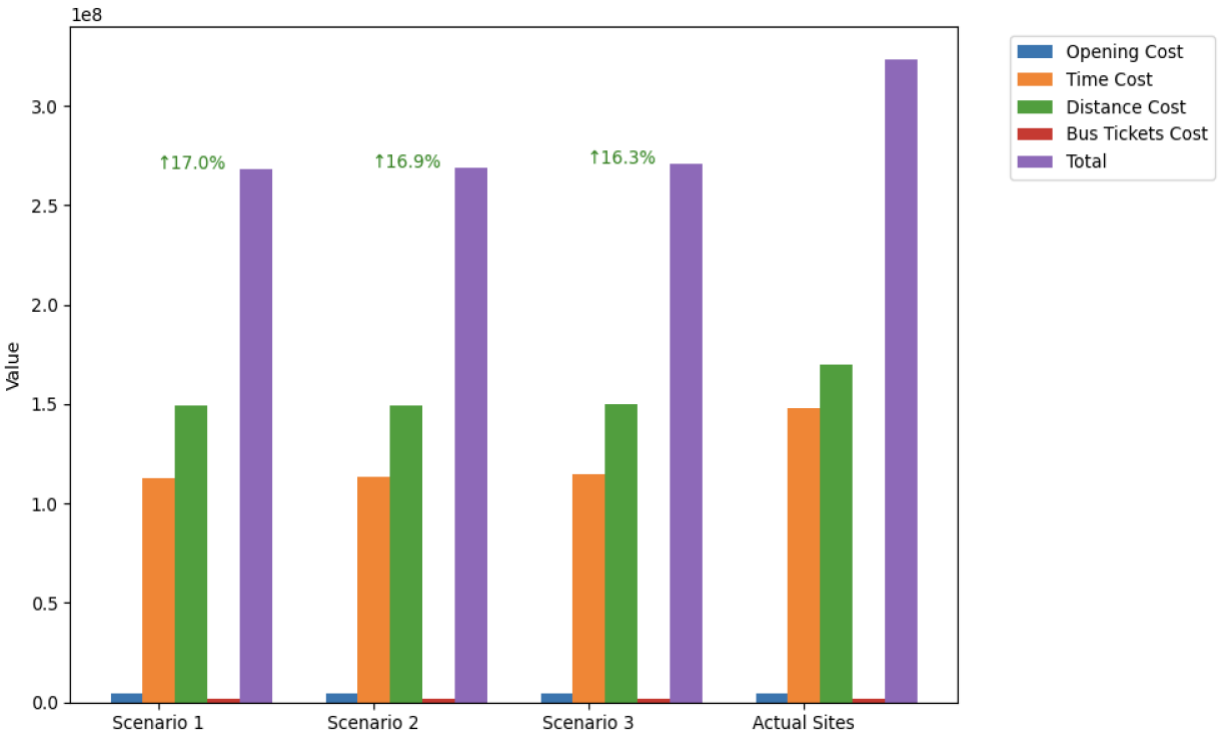

Figure 9: Cost types comparison

- **When F=1:**

Similarly, we compared the three scenarios to the actual sites when F=1. This yielded an even larger gap between the proposed sites by the model than the true sites selected in LA County, as can be seen in the following charts that show the comparisons in average travel times and distance as well as the total costs:

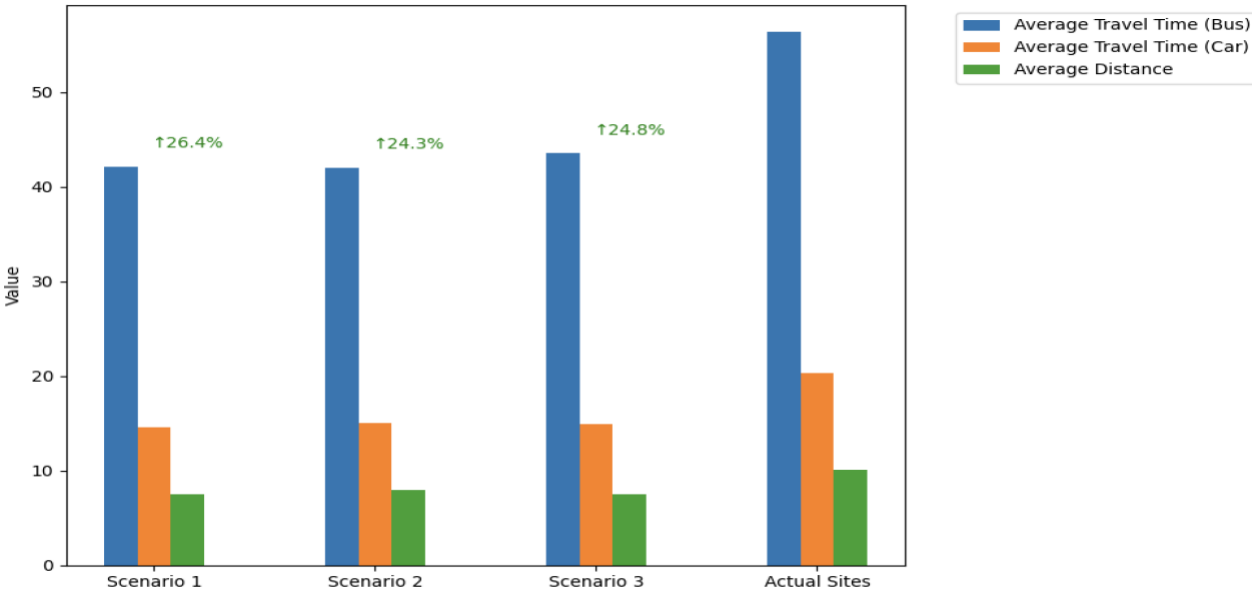

Figure 10: Average travel times and distance comparison

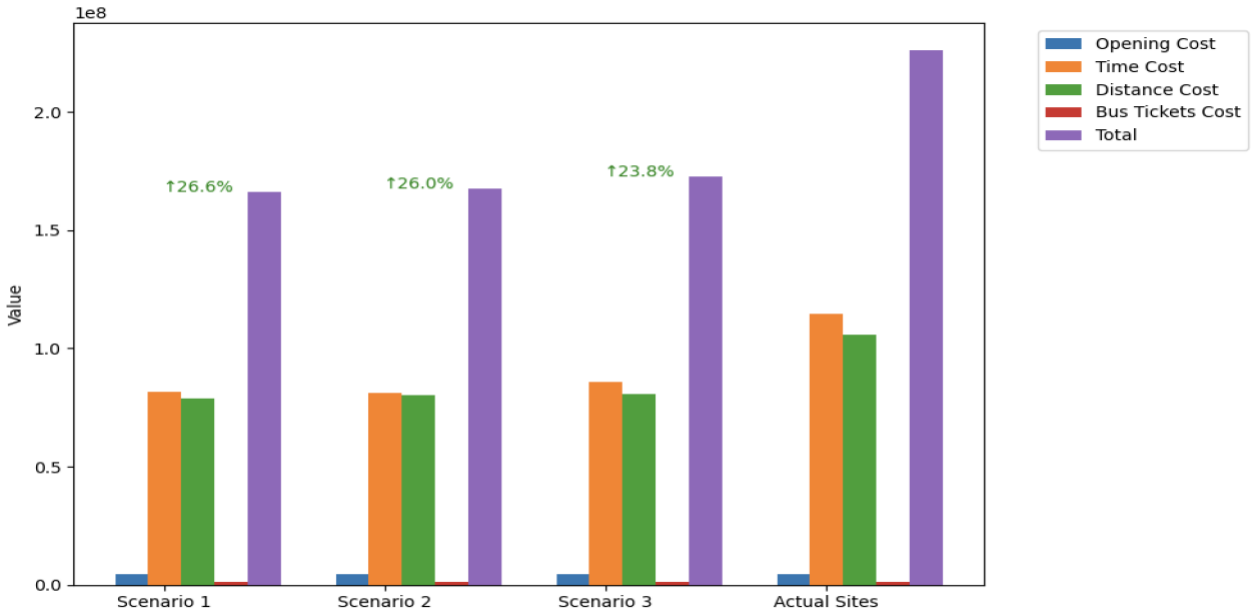

Figure 11: Cost types comparison

5.5 Limitations

This thesis provided valuable insights into the optimization of vaccine distribution centers and vaccine allocation. However, it is important to acknowledge certain limitations that may have limited the work, such as in the estimation of site opening costs, and COVID-19 data availability on zip codes level.

One of the key assumptions in the model is the cost of opening a vaccination site, which is roughly estimated to be $500,000. This number is general approximation and does not consider the variability in actual real estate's costs across different areas within the LA County. The actual cost of establishing vaccination sites can vary significantly depending on the location, size, and other factors such as rental, renovation and operational costs. Therefore, the interpretation of results of the model should consider this limitation in mind. Future research could build on this aspect by conducting a more precise cost analysis.

Another limitation in the study is the lack of certain COVID-19 data on the zip code level. Data on COVID-19 cases and deaths are only available and consolidated on district/community level, which could not be accurately converted to the zip code level. The model could potentially yield better results and explore the problem from different angles given the availability of such data.

Chapter Six: Conclusion.

6.1 Summary of Findings.

This thesis studied the selection of COVID-19 vaccine distribution centers, allocation quantities, and associated costs within the County of Los Angeles. The study, using a Mixed Integer Programming model, explored three different scenarios based on the following prioritization techniques:

- Priority assignment based on population.
- Priority assignment based on the California Healthy Places Index (HPI).
- Priority assignment based on a COVID-19 Vulnerability index.

The model assumed that up to 20 sites could be selected, with a limited budget of $10M.

The first scenario, using the population as a weighting factor, yielded the lowest costs, which came to a total of $194,815,902. Moreover, the average travel time by car and transit, as well as the distance traveled between the selected sites and the 277 zip code, were also the lowest for this scenario. The average travel times were 47.4 min and 16 min for transit and car users, respectively. The average distance was 9 miles. Since priorities were given based on populations, the selected sites appear to be close to the highly populated sides of the County. This suggests that prioritizing areas with higher populations can lead to be more cost-efficient.

For the second scenario, the optimal weighted costs were $196,402,988. The average travel times and distance were the highest among the three, with 48.9 min for transit, 16.3 min for car, and 9.3 miles for distance. The selected sites were very close to zip codes with a wide range of HPI percentiles, from as low as 0.032 to 0.55. This range suggests that the model selected a diverse set of sites, with the majority being on the lower side of percentiles. This indicates while prioritizing

areas based on the HPI can lead to a more diverse locations, it might also result in higher costs and travel times due to the broader spread of these areas.

The last scenario yielded the highest weighted total cost of all, with a total cost of $200,034,495, while resulting in average times and distances of 48.5 min for transit, 16.2 min for car, and 9 miles. This highlights the potential trade-off between prioritizing areas with high vulnerability and the increase in the associated costs and travel times.

After comparing the results of the three scenarios, it becomes clear that different prioritization techniques have a significant impact on the outcomes, which highlights the importance of careful consideration during the deciding-making and planning process.

The sensitivity analysis explored changing the maximum number of sites to up to 40 sites and changing the number of choices people have for taking the vaccines from a single site to 5 sites. The findings showed that the total costs decreased as the number of sites increased, primarily due to the time and distance expenses constituting the bulk of costs. The results also showed that as the number of site choices (F) decreases, the geographic spread of the sites is increased.

In Conclusion, the developed model in this thesis introduces innovative approaches to solving the problem of optimizing vaccination centers. The model is designed to account for multiple factors, such as minimizing the travel time and distance between residential areas and supply points of limited resources and their associated costs. It also takes into account socioeconomic and demographic factors, allowing for the assignment of priority to areas based on chosen criteria. Furthermore, the model assumes that individuals will travel to the closest vaccination site, but in reality, they may select from multiple sites based on preference. The model gives this flexibility to the people. However, our findings suggest that this might lead to a less optimal solution

accompanied by a decrease in the spread of the selected sites. Finally, the application of the model to Los Angeles County, which is one of the largest and most diverse counties in the United States, demonstrates its flexibility and effectiveness.

Overall, our findings highlight the trade-offs involved in the selection of vaccination sites and the benefits of using an optimization model to inform this process.

6.2 Contributions to the Field.

This research contributes to the ongoing efforts to manage and battle rapid evolving global pandemics, particularly in managing the selection of distribution centers of scarce resources. By taking into account various factors for assigning priority, policy and decision-makers can choose the option that best fits the specific characteristics of the pandemic, the study area and its populations.

The findings of the research have practical implications that could improve public health outcomes. They offer valuable insights that can give guidance and recommendations to the authorities in making informed decisions about the strategic selection of distribution centers and how to allocate resources. This would lead to better use of resources, reduced travel times for individuals, and consequently, higher vaccination rates and reduced deaths.

By optimizing the locations of the COVID-19 centers, we hope to save not only resources, but also lives. Efficient distribution leads to better control of the pandemic, more protected communities, and a quicker return to normal life and economic activities.

6.3 Future Research.

Future research could build on this thesis by incorporating additional factors into the optimization process of vaccine centers. This could include an in-depth analysis of the staffing requirements, the process of administering the vaccines and optimizing the capacity of each distribution center. Additionally, the cost analysis associated with establishing these sites is by itself a substantial area of study. Future studies could explore this aspect deeper, developing a dynamic approach that considers all factors involved in estimating the costs of opening health facilities. Examples of those factors could be real estate costs, construction costs, equipment, and supply costs.

In conclusion, the potential for research in this field is vast, and by exploring those ideas, we can continue to refine our approaches and improve the efficiency and effectiveness of public health outcomes.

References

[1] “Covid-19 Vaccine .” LA County COVID-19 Vaccine Dashboard - LA County Department of Public Health, publichealth.lacounty.gov/media/coronavirus/vaccine/vaccine-dashboard.htm. Accessed 13 May 2023.

[2] Mollalo, Abolfazl et al. “Spatial Analysis of COVID-19 Vaccination: A Scoping Review.” International journal of environmental research and public health vol. 18,22 12024. 16 Nov. 2021, doi:10.3390/ijerph182212024

[3] Mollalo, Abolfazl, and Moosa Tatar. “Spatial Modeling of COVID-19 Vaccine Hesitancy in the United States.” International journal of environmental research and public health vol. 18,18 9488. 8 Sep. 2021, doi:10.3390/ijerph18189488

[4] Krzysztofowicz, Sylwia, and Katarzyna Osińska-Skotak. “The Use of GIS Technology to Optimize COVID-19 Vaccine Distribution: A Case Study of the City of Warsaw, Poland.” International journal of environmental research and public health vol. 18,11 5636. 25 May. 2021, doi:10.3390/ijerph18115636

[5] Alemdar, Kadir Diler, et al. “Accessibility of Vaccination Centers in COVID-19 Outbreak Control: A GIS-Based Multi-Criteria Decision Making Approach.” ISPRS International Journal of Geo-Information, vol. 10, no. 10, Oct. 2021, p. 708. Crossref, https://doi.org/10.3390/ijgi10100708.

[6] Cheng, Min et al. “Measuring Spatial Accessibility of Urban Medical Facilities: A Case Study in Changning District of Shanghai in China.” International journal of environmental research and public health vol. 18,18 9598. 12 Sep. 2021, doi:10.3390/ijerph18189598

[7] Bravo, Fernanda and Hu, Jingyuan and Long, Elisa, Closer to Home: Partnering to Distribute Vaccinations under Spatially Heterogeneous Demand (February 6, 2023). Available at SSRN: https://ssrn.com/abstract=4008669 or http://dx.doi.org/10.2139/ssrn.4008669

[8] Bravo, Fernanda and Hu, Jingyuan and Long, Elisa, Closer to Home: Partnering to Distribute Vaccinations under Spatially Heterogeneous Demand (February 6, 2023). Available at SSRN: https://ssrn.com/abstract=4008669 or http://dx.doi.org/10.2139/ssrn.4008669

[9] Risanger, Simon et al. “Selecting pharmacies for COVID-19 testing to ensure access.” Health care management science vol. 24,2 (2021): 330-338. doi:10.1007/s10729-020-09538-w

[10] Bertsimas, Dimitris, et al. “Where to Locatecovid-19 Mass Vaccination Facilities?” Naval Research Logistics (NRL), vol. 69, no. 2, 2021, pp. 179–200, https://doi.org/10.1002/nav.22007.

[11] Alghanmi, Nusaybah et al. “A Survey of Location-Allocation of Points of Dispensing During Public Health Emergencies.” Frontiers in public health vol. 10 811858. 10 Mar. 2022, doi:10.3389/fpubh.2022.811858

[12] Lusiantoro, Luluk, et al. “A Locational Analysis Model of the COVID-19 Vaccine Distribution.” Operations and Supply Chain Management: An International Journal, Apr. 2022, pp. 240–50, https://doi.org/10.31387/oscm0490344. Accessed 12 June 2022.

[13] Tang, Lianhua et al. “Bi-objective optimization for a multi-period COVID-19 vaccination planning problem.” Omega vol. 110 (2022): 102617. doi:10.1016/j.omega.2022.102617

[14] Cabanilla, Kurt Izak et al. “Optimal selection of COVID-19 vaccination sites in the Philippines at the municipal level.” PeerJ vol. 10 e14151. 30 Sep. 2022, doi:10.7717/peerj.14151

[15] Alhothali, Areej et al. “Location-Allocation Model to Improve the Distribution of COVID-19 Vaccine Centers in Jeddah City, Saudi Arabia.” International journal of environmental research and public health vol. 19,14 8755. 19 Jul. 2022, doi:10.3390/ijerph19148755

[16] Karmakar, Monita, et al. “Association of Social and Demographic Factors with COVID-19 Incidence and Death Rates in the US.” JAMA Network Open, vol. 4, no. 1, 29 Jan. 2021, p. e2036462, https://doi.org/10.1001/jamanetworkopen.2020.36462.

[17] Ong, Paul M et al. “COVID-19 Medical Vulnerability Indicators: A Predictive, Local Data Model for Equity in Public Health Decision Making.” International journal of environmental research and public health vol. 18,9 4829. 30 Apr. 2021, doi:10.3390/ijerph18094829

[18] Burcu Balcik, et al. A Mathematical Model for Equitable In-Country COVID-19 Vaccine Allocation. Vol. 60, no. 24, 18 Aug. 2022, pp. 7502–7526, https://doi.org/10.1080/00207543.2022.2110014. Accessed 13 June 2023.

[19] Anahideh, Hadis et al. “Fair and diverse allocation of scarce resources.” Socioeconomic planning sciences vol. 80 (2022): 101193. doi:10.1016/j.seps.2021.101193

[20] Wang, Zhennan, "Equitable Distribution of Covid-19 Vaccines: Can Data Visualization and Optimization Help?" (2021). Honors College Theses. 328. https://digitalcommons.pace.edu/honorscollege_theses/328

[21] Singh, Bismark. “Fairness Criteria for Allocating Scarce Resources.” Optimization Letters, 13 Mar. 2020, https://doi.org/10.1007/s11590-020-01568-1. Accessed 27 Apr. 2023.

[22] Buhat, Christian Alvin H et al. “Using Constrained Optimization for the Allocation of COVID-19 Vaccines in the Philippines.” Applied health economics and health policy vol. 19,5 (2021): 699-708. doi:10.1007/s40258-021-00667-z

[23] Babus, Ana et al. “The optimal allocation of Covid-19 vaccines.” Economics letters vol. 224 (2023): 111008. doi:10.1016/j.econlet.2023.111008

[24] Fadaki, Masih et al. “Multi-period vaccine allocation model in a pandemic: A case study of COVID-19 in Australia.” Transportation research. Part E, Logistics and transportation review vol. 161 (2022): 102689. doi:10.1016/j.tre.2022.102689

[25] Bertsimas, Dimitris & Ivanhoe, Joshua & Jacquillat, Alexandre & Li, Michael & Previero, Alessandro & Lami, Omar & Bouardi, Hamza. (2020). Optimizing Vaccine Allocation to Combat the COVID-19 Pandemic. 10.1101/2020.11.17.20233213.

[26] Haouari, Mohamed, and Mariem Mhiri. "A particle swarm optimization approach for predicting the number of COVID-19 deaths." Scientific reports vol. 11,1 16587. 16 Aug. 2021, doi:10.1038/s41598-021-96057-5

[27] Alberti, Tommaso, and Davide Faranda. "On the uncertainty of real-time predictions of epidemic growths: A COVID-19 case study for China and Italy." Communications in nonlinear science & numerical simulation vol. 90 (2020): 105372. doi:10.1016/j.cnsns.2020.105372

[28] Emu, Mahzabeen & Chandrasekaran, Dhivya & Mago, Vijay & Choudhury, Salimur. (2021). Validating Optimal COVID-19 Vaccine Distribution Models. 10.1007/978-3-030-77961-0_30.

[29] "California Healthy Places Index." Map.healthyplacesindex.org, map.healthyplacesindex.org/?redirect=false.

[30] CDC. "Coronavirus Disease 2019 (COVID-19)." Centers for Disease Control and Prevention, 11 Feb. 2020, www.cdc.gov/coronavirus/2019-ncov/covid-data/investigations-discovery/hospitalization-death-by-age.html. Accessed 20 March. 2023

[31] "Explore Census Data." Data.census.gov, data.census.gov/table?g=040XX00US06_1400000US06037101122_050XX00US06037. Accessed 15 March 2023.

[32] "Revised Departmental Guidance on Valuation of Travel Time in Economic Analysis | US Department of Transportation." Www.transportation.gov, www.transportation.gov/office-policy/transportation-policy/revised-departmental-guidance-valuation-travel-time-economic.

[33] "Auto Club: SoCal Driving Costs Six Percent Higher than US Average." AAA SoCal, 8 May 2015, news.aaa-calif.com/news/auto-club:-socal-driving-costs-six-percent-higher-than-us-average. Accessed 10 April 2023.

[34] Maizlish, Neil et al. "California Healthy Places Index: Frames Matter." Public health reports (Washington, D.C. : 1974) vol. 134,4 (2019): 354-362. doi:10.1177/0033354919849882

[35] "LA County COVID-19 Vaccine Dashboard - LA County Department of Public Health." Publichealth.lacounty.gov,publichealth.lacounty.gov/media/Coronavirus/vaccine/vaccine-dashboard.htm. Accessed 10 April. 2023

[36] "Explore Census Data." Data.census.gov, data.census.gov/map?g=040XX00US06&tid=ACSDP5Y2020.DP04&cid=DP04_0057E&layer=VT_2020_860_Z2_PY_D1&mode=thematic&loc=33.5590. Accessed 1 December 2022.

[37] “City of Los Angeles Hub.” Geohub.lacity.org, geohub.lacity.org/. Accessed 20 November. 2022

[38] Staff and wire reports •. “List: SoCal Coronavirus Vaccination Super-Sites.” NBC Los Angeles, 14 Jan. 2021, www.nbclosangeles.com/news/local/list-socal-super-coronavirus-vaccination-sites/2506311/. Accessed 5 June 2023.

Appendix

- **Sensitivity Analysis Plots for Scenario 2**

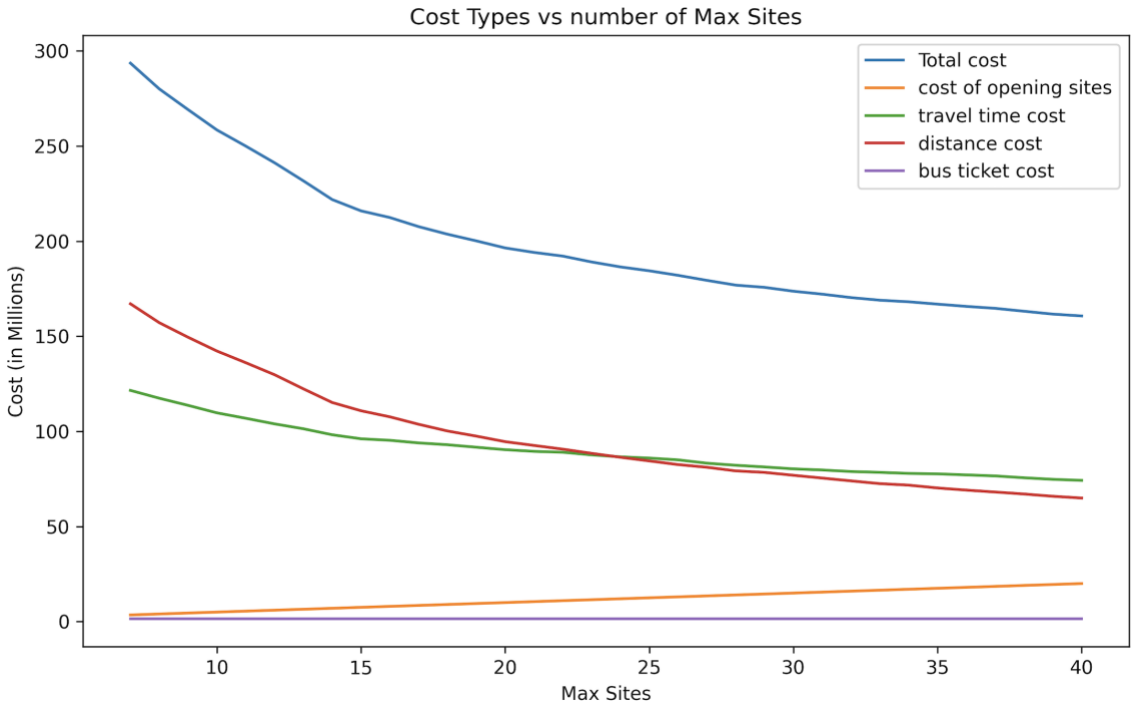

Figure 12: Cost types vs max sites for scenario 2

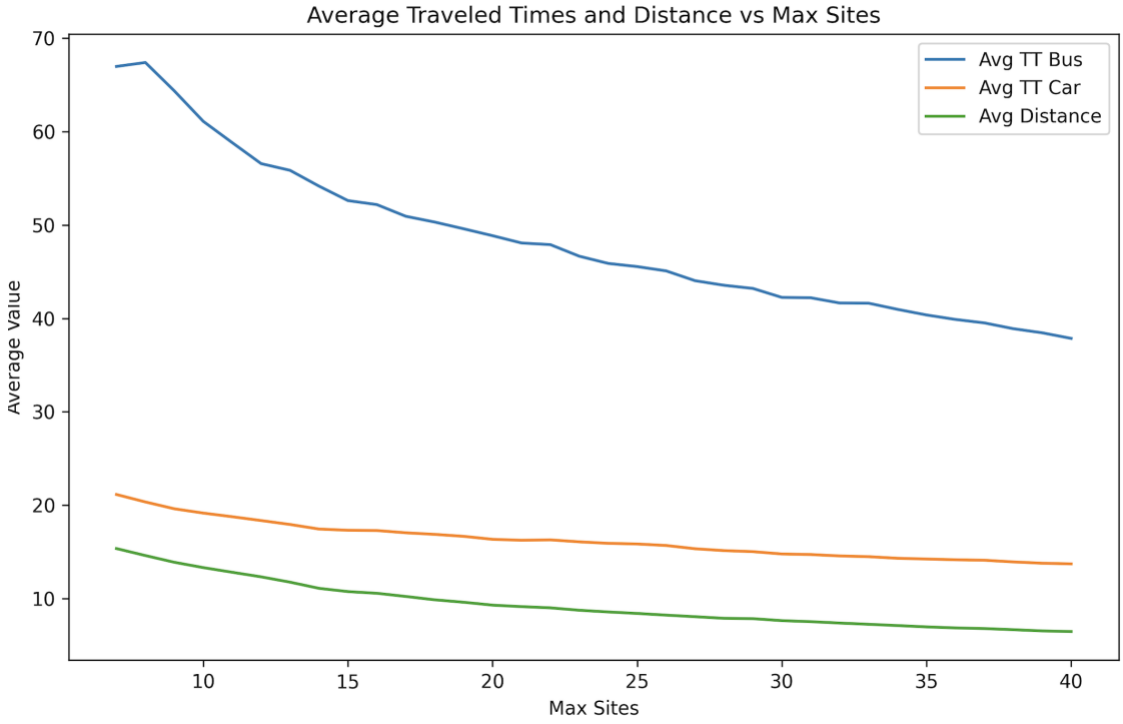

Figure 13: Average travel times and distance vs max sites for scenario 2

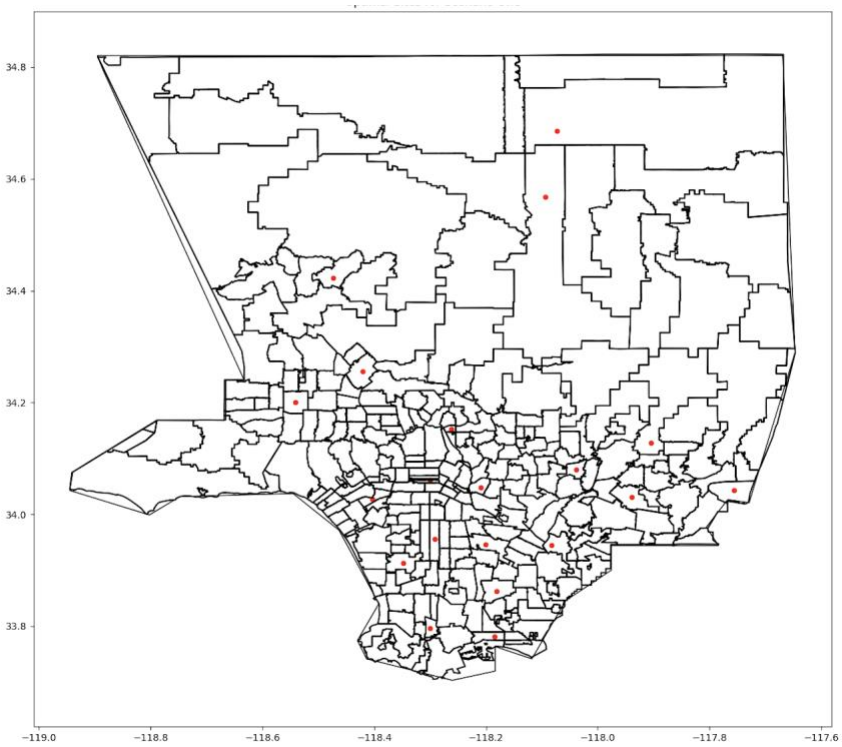

Map 11: Map of selected sites when F=1, scenario 2

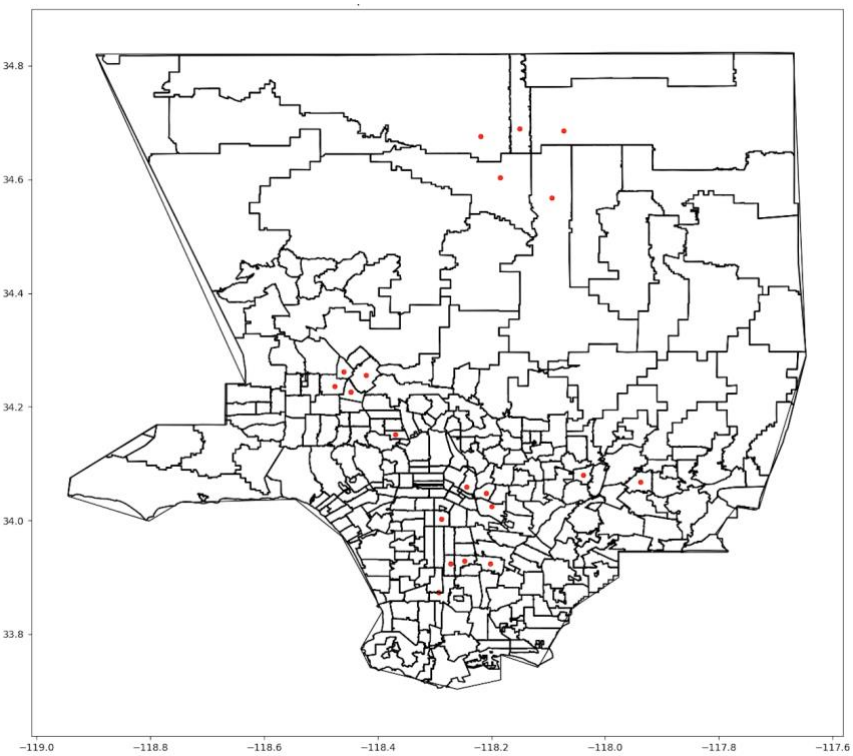

Map 12: Map of selected sites when F=5, scenario 2

- **Sensitivity Analysis Plots for Scenario 3**

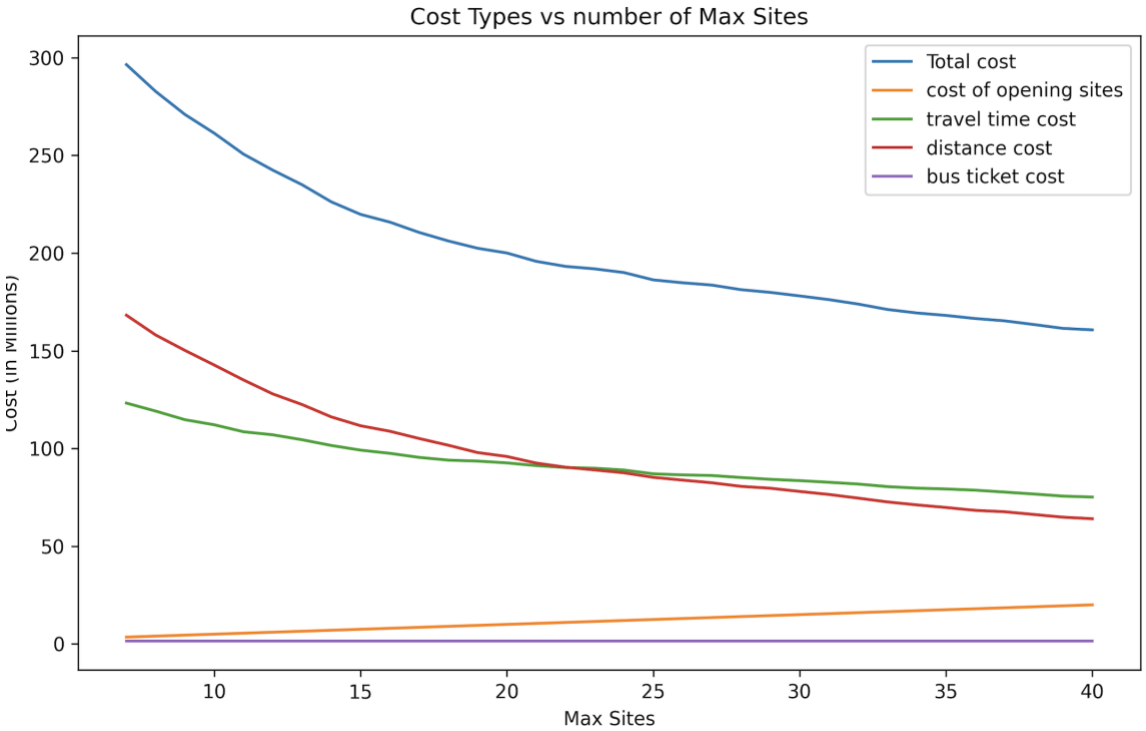

Figure 14: Cost types vs max sites for scenario 3

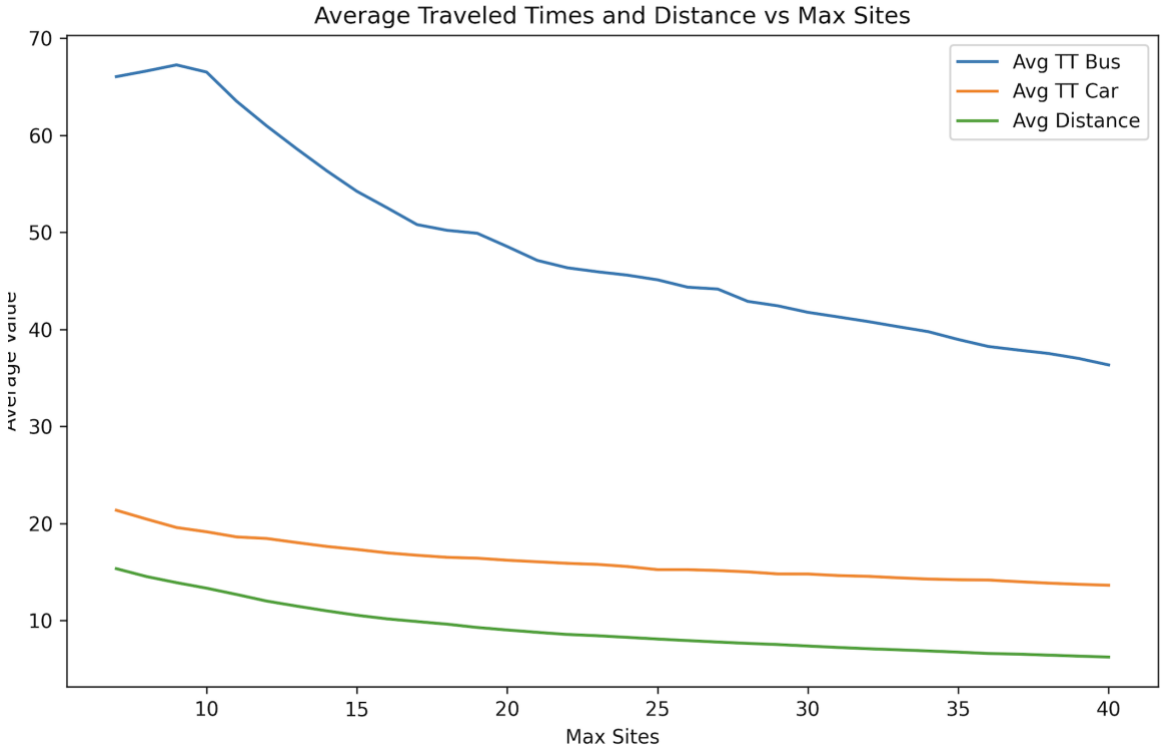

Figure 15: Average travel times and distance vs max sites for scenario 2

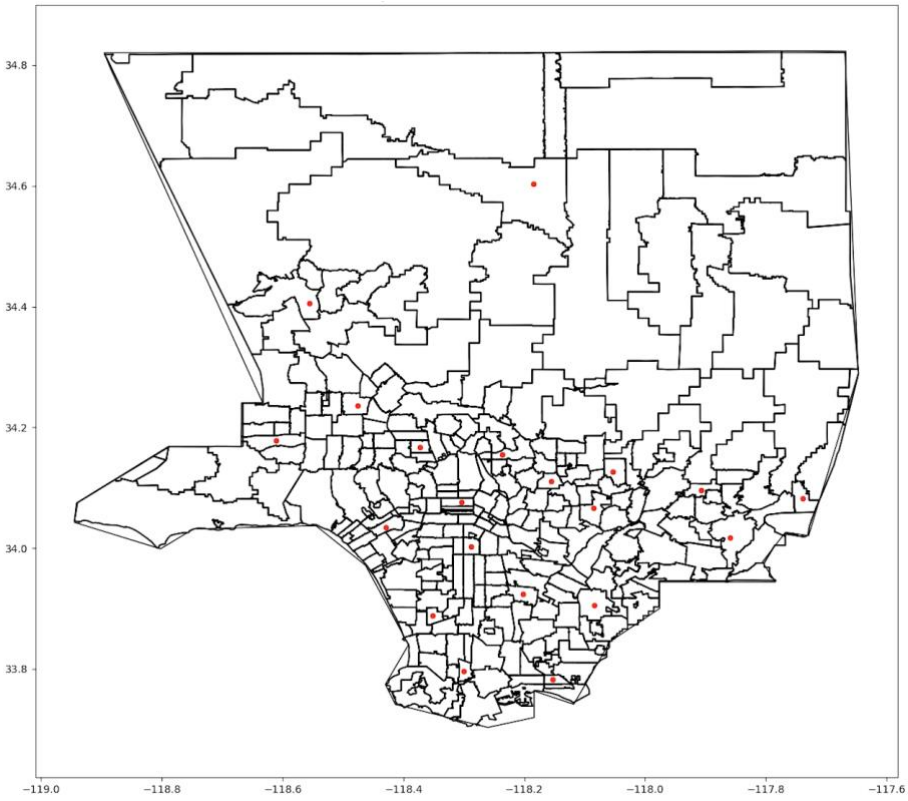

Map 13: Optimal sites for F=1, scenario 3

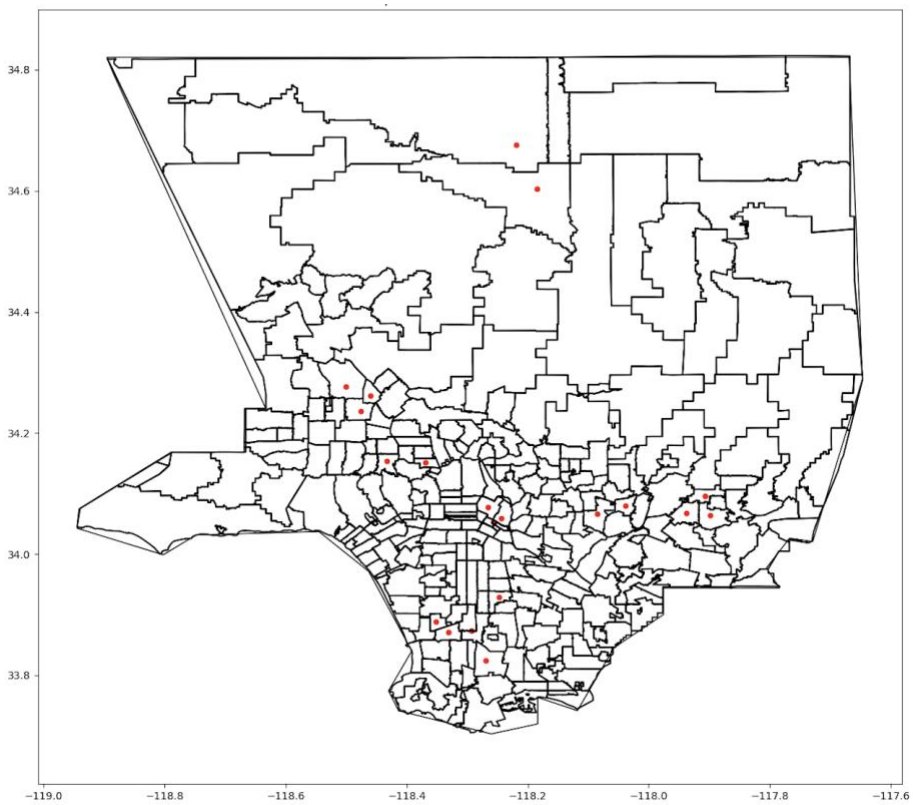

Map 14: Optimal sites for F=5, scenario 3

max_sites	Z	Total cost	cost of opening sites	travel time cost	distance cost	bus tickets cost	Avg TT Bus	Avg TT Car	Avg Distance
7	293530630	293530630.6	3500000	121517011.4	167027723.2	1485895.97	66.99	21.14	15.35
8	279588541	279588541.3	4000000	116979361.3	157123284.1	1485895.97	67.8	20.11	14.6
9	268525699	268525700	4500000	113075508	149464296	1485895.97	64.55	19.61	13.93
10	257748481	257748481.7	5000000	109408872.6	141853713.1	1485895.97	61.36	19.01	13.24
11	248222650	248222650.9	5500000	106806783	134429972	1485895.97	60.53	18.58	12.67
12	238917314	238917314.4	6000000	104010059.8	127421358.6	1485895.97	57.94	18.12	12.05
13	230139102	230139102.5	6500000	100606998.1	121546208.5	1485895.97	55.47	17.75	11.56
14	221572843	221572843.9	7000000	97661968.69	115424979.3	1485895.97	53.34	17.35	11.09
15	215072181	215072181.7	7500000	96398286.08	109687999.7	1485895.97	52.67	17.28	10.59
16	209845679	209845679.3	8000000	94493547.33	105866236	1485895.97	52.04	16.92	10.27
17	205491821	205491821.5	8500000	93139869.8	102366055.8	1485895.97	50.17	16.69	9.85
18	201617936	201617936.5	9000000	91694275.72	99437764.76	1485895.97	49.11	16.46	9.63
19	198000598	198000598.7	9500000	90670525.99	96344176.73	1485895.97	48	16.25	9.27
20	194815902	194815903	10000000	89647526.18	93682480.82	1485895.97	47.44	15.99	9.01
21	191716863	191716863.9	10500000	88152370.94	91578597.01	1485895.97	47.09	15.75	8.84
22	188998579	188998579.3	11000000	86978129.04	89534554.3	1485895.97	46.12	15.59	8.68
23	186298834	186298834.6	11500000	86232898.41	87080040.25	1485895.97	45.38	15.51	8.47

max_sites	Z	Total cost	cost of opening sites	travel time cost	distance cost	bus tickets cost	Avg TT Bus	Avg TT Car	Avg Distance
24	183851856	183851856.2	12000000	85259681.59	85106278.59	1485895.97	44.71	15.34	8.28
25	181461824	181461824.2	12500000	84437526.85	83038401.34	1485895.97	43.62	15.18	8.04
26	179428133	179428133.1	13000000	83514212.29	81428024.81	1485895.97	43.26	15.1	7.95
27	177369678	177369678.9	13499999.98	82952355.99	79431426.92	1485895.97	42.69	15.03	7.7
28	175430677	175430677.2	14000000	82443665.9	77501115.34	1485895.97	42.26	14.97	7.53
29	173550073	173550073.4	14500000	81753489.44	75810688.03	1485895.97	41.8	14.89	7.41
30	171864627	171864627.8	15000000	80967791.81	74410940.06	1485895.97	41.43	14.77	7.29
31	170209903	170209903.3	15500000	79818782.47	73405224.83	1485895.97	40.71	14.46	7.17
32	168613105	168613105.8	16000000	79126310.24	72000899.56	1485895.97	39.53	14.35	7
33	167027225	167027225.7	16499999.96	79231554.4	69809775.37	1485895.97	39.54	14.41	6.83
34	165564549	165564549.6	17000000	78637194.97	68441458.63	1485895.97	38.54	14.35	6.7
35	164154071	164154071.6	17500000	78089564.11	67078611.5	1485895.97	38.21	14.19	6.54
36	162787398	162787398.8	18000000	76850483.09	66451019.7	1485895.97	37.22	14.02	6.48
37	161525057	161525057.2	18500000	76299826.73	65239334.46	1485895.97	37.13	13.9	6.37
38	160303115	160303115	19000000	75864339.31	63952879.72	1485895.97	36.53	13.82	6.25
39	159110460	159110460.9	19500000	74885096.98	63239467.94	1485895.97	36.5	13.68	6.21
40	158010146	158010146.9	20000000	73951317.96	62572932.97	1485895.97	36.28	13.58	6.17

Table 15: Loop output for scenario 1

max_sites	Z	Total cost	cost of opening sites	travel time cost	distance cost	bus tickets cost	Avg TT Bus	Avg TT Car	Avg Distance
7	314211669	293530630.6	3500000	121517011.4	167027723.2	1485895.97	66.99	21.14	15.35
8	299398750	279985724.3	4000000	117398384.2	157101444.2	1485895.97	67.41	20.34	14.6
9	286479444	269083845.3	4500000	113650807.8	149447141.6	1485895.97	64.37	19.61	13.88
10	274343273	258398982.1	5000000	109708996.7	142204089.4	1485895.97	61.11	19.15	13.31
11	262678555	249923842.2	5500000	106862097	136075849.2	1485895.97	58.83	18.76	12.81
12	251048330	241153704.3	6000000	103915245.4	129752563	1485895.97	56.58	18.35	12.32
13	240835696	231661498.8	6500000	101346781	122328821.8	1485895.97	55.86	17.93	11.75
14	231018316	221820172.4	7000000	98190615.63	115143660.8	1485895.97	54.17	17.44	11.09
15	223104384	215873639.5	7500000	96078846.63	110808896.9	1485895.97	52.62	17.31	10.74
16	218298607	212382499.6	8000000	95281388.9	107615214.7	1485895.97	52.19	17.28	10.56
17	214149173	207591078.3	8500000	93908006.21	103697176.1	1485895.97	50.94	17.04	10.22
18	210609335	203609589.5	9000000	92950486.92	100173206.6	1485895.97	50.32	16.87	9.86
19	207305505	200106839.5	9500000	91642610.01	97478333.56	1485895.97	49.6	16.66	9.6
20	204038094	196402988.7	10000000	90351438.72	94565654.05	1485895.97	48.86	16.34	9.29
21	200899577	194043569.9	10500000	89475241.72	92582432.23	1485895.97	48.08	16.24	9.13
22	197902306	192108864.1	11000000	88993072.58	90629895.53	1485895.97	47.9	16.28	9
23	195081310	189017913.2	11500000	87610028.22	88421989.02	1485895.97	46.66	16.07	8.74

max_sites	Z	Total cost	cost of opening sites	travel time cost	distance cost	bus tickets cost	Avg TT Bus	Avg TT Car	Avg Distance
24	192375526	186415764.6	12000000	86576423.75	86353444.82	1485895.97	45.89	15.91	8.56
25	190008978	184380838.4	12500000	85953573.89	84441368.56	1485895.97	45.55	15.84	8.4
26	187780472	181994637.6	13000000	84994226.71	82514514.94	1485895.97	45.09	15.68	8.22
27	185755249	179345970.7	13500000	83255004.9	81105069.84	1485895.97	44.04	15.33	8.05
28	183844659	176846056.5	14000000	82155139.58	79205020.99	1485895.97	43.55	15.13	7.88
29	181987018	175677568.6	14500000	81277567.87	78414104.71	1485895.97	43.21	15.02	7.84
30	180132736	173645993.6	15000000	80264633.03	76895464.56	1485895.97	42.25	14.77	7.63
31	178398604	172102178.9	15500000	79686707.96	75429574.95	1485895.97	42.21	14.71	7.52
32	176821580	170302270.2	16000000	78866442.07	73949932.14	1485895.97	41.65	14.56	7.37
33	175309097	168925657.8	16500000	78436800.24	72502961.55	1485895.97	41.63	14.48	7.24
34	173969220	168091427.8	17000000	77888860.64	71716671.22	1485895.97	40.97	14.31	7.1
35	172629280	166859124	17500000	77638292.11	70234935.94	1485895.97	40.37	14.23	6.96
36	171310679	165676178.3	18000000	77093154.74	69097127.61	1485895.97	39.89	14.15	6.85
37	169991849	164653428.8	18499999.97	76568110.01	68099422.8	1485895.97	39.52	14.1	6.78
38	168689571	163130837.9	19000000	75584774.95	67060166.99	1485895.97	38.9	13.92	6.66
39	167464712	161621325.6	19500000	74774834.74	65860594.87	1485895.97	38.46	13.78	6.53
40	166326531	160656541.6	20000000	74223757.9	64946887.74	1485895.97	37.86	13.71	6.46

Table 16: Loop output for scenario 2

max_sites	Z	Total cost	cost of opening sites	travel time cost	distance cost	bus tickets cost	Avg TT Bus	Avg TT Car	Avg Distance
7	272518936	296432268.1	3500000	123239473.6	168206898.5	1485895.97	66.04	21.35	15.33
8	259432668	282696790.6	4000000	119137094.2	158073800.5	1485895.97	66.62	20.44	14.52
9	247834993	270909716	4500000	114733249.1	150190570.9	1485895.97	67.25	19.57	13.89
10	239132641	261339460.2	5000000	112140280.9	142713283.3	1485895.97	66.51	19.13	13.32
11	231007504	250628829.2	5500000	108569289.8	135073643.5	1485895.97	63.5	18.6	12.67
12	222888181	242435503.4	6000000	107018225.1	127931382.3	1485895.97	60.96	18.44	11.99
13	215949395	234976532.5	6500000	104491506.8	122499129.8	1485895.97	58.6	18.02	11.47
14	209284336	226204524.5	7000000	101553045.7	116165582.8	1485895.97	56.33	17.62	10.98
15	203221875	219795156.9	7500000	99168651.23	111640609.7	1485895.97	54.22	17.31	10.53
16	198213948	215842409.4	8000000	97524969.6	108831543.8	1485895.97	52.53	16.96	10.16
17	193748988	210566254.3	8500000	95457957.96	105122400.4	1485895.97	50.79	16.71	9.88
18	189552500	206187462.2	9000000	94045187.68	101656378.6	1485895.97	50.2	16.5	9.61
19	185816922	202458300.1	9500000	93563661.08	97908743.01	1485895.97	49.9	16.41	9.27
20	182327956	200034495	10000000	92633900.93	95914698.13	1485895.97	48.53	16.2	9.01
21	179071687	195771582.1	10500000	91241544.25	92544141.92	1485895.97	47.1	16.04	8.77
22	176161853	193190691	11000000	90272135.57	90432659.47	1485895.97	46.34	15.88	8.55
23	173470468	191917763.9	11500000	89914408.69	89017459.24	1485895.97	45.93	15.77	8.42

max_sites	Z	Total cost	cost of opening sites	travel time cost	distance cost	bus tickets cost	Avg TT Bus	Avg TT Car	Avg Distance
24	170843273	190025850.9	12000000	88981869.2	87558085.73	1485895.97	45.58	15.55	8.25
25	168479525	186274011.9	12500000	87048394.54	85239721.36	1485895.97	45.1	15.23	8.08
26	166322155	184806913.4	13000000	86492379.48	83828637.9	1485895.97	44.34	15.23	7.92
27	164269358	183621917.9	13500000	86173194.03	82462827.9	1485895.97	44.15	15.14	7.77
28	162363575	181269222.8	14000000	85160921.11	80622405.74	1485895.97	42.88	15	7.63
29	160533065	179882639.4	14500000	84231276.77	79665466.65	1485895.97	42.42	14.79	7.51
30	158789947	178072999.3	15000000	83562419.15	78024684.19	1485895.97	41.75	14.78	7.36
31	157065371	176182611.6	15500000	82719288.68	76477426.95	1485895.97	41.28	14.62	7.21
32	155461116	173905567.7	16000000	81815308.17	74604363.58	1485895.97	40.8	14.54	7.08
33	153979662	171141715.7	16500000	80499124.44	72656695.28	1485895.97	40.27	14.39	6.97
34	152495413	169354502.4	17000000	79723248.13	71145358.29	1485895.97	39.76	14.26	6.85
35	151182940	168092379.8	17500000	79289602.92	69816880.91	1485895.97	38.95	14.19	6.73
36	149871223	166508626.5	18000000	78681406.59	68341323.9	1485895.97	38.23	14.16	6.59
37	148704289	165331589.6	18500000	77707086.49	67638607.16	1485895.97	37.86	13.99	6.52
38	147571611	163438406.2	19000000	76710982.62	66241527.57	1485895.97	37.51	13.84	6.42
39	146468145	161467432.8	19500000	75633591.22	64847945.63	1485895.97	37	13.72	6.32
40	145406585	160710235.1	20000000	75163378.84	64060960.29	1485895.97	36.33	13.62	6.22

Table 17: Loop output for scenario 3